2009

Estimating age at death by examining the crystallite size of hydroxylapatite in human teeth

Teresa Veronica Wilson
Louisiana State University and Agricultural and Mechanical College, teresavwilson@gmail.com

ESTIMATING AGE AT DEATH BY EXAMINING THE CRYSTALLITE SIZE OF HYDROXYLAPATITE IN HUMAN TEETH

A Thesis

Submitted to the Graduate Faculty of the
Louisiana State University and
Agricultural and Mechanical College
in partial fulfillment of the
requirements for the degree of
Master of Arts

in

The Department of Geography and Anthropology

by
Teresa Veronica Wilson
B.A., Northern Arizona University, 2007
May 2009

ACKNOWLEDGEMENTS

I wish to thank my thesis committee for all of their encouragement and support. I am eternally indebted to my advisor, Ms. Mary Manhein, for always believing in this project and for permitting me to venture into the unknown. I thank her for her enthusiasm and for all of the opportunities that she has given me during my time at Louisiana State University. I am appreciative of Dr. Ray Ferrell for his patience and vast knowledge of x-ray diffraction. This thesis would not have been possible without his interest in my research and his willingness to provide the instruments needed for this research. I want to thank Dr. Rebecca Saunders for her sincere interest in this endeavor and for keeping me grounded.

I would like to thank the Department of Geology and Geophysics at Louisiana State University and the X-Ray Diffraction Laboratory for allowing me to use their facilities during the course of this research. I am grateful to Mrs. Wanda LeBlanc for her unending help with sample preparation and for providing a lending hand when things did not always go as planned. I could not have completed the analysis without her assistance and patience while I was learning how to use Jade.

This research was funded in part by the Department of Geography and Anthropology at Louisiana State University. I would like to thank the Forensic Anthropology and Computer Enhancement Services (FACES) Laboratory at Louisiana State University for allowing me to collect samples from the comparative collection and for the use of their photographic equipment.

Thank you to all of my friends at LSU who did not let me become overwhelmed and helped to me to see the bigger picture. A special thank you goes to Ms. Lauren Pharr for letting me use one of her thesis specimens in my research, which offered a unique opportunity to collect samples from a skeletal pig of known age.

Last but not least, I would like to thank my husband, Jonathan Wilson, for supporting my decision to go to graduate school and moving all the way to Louisiana so that I could pursue my dream. Thank you for never letting me give up and always pushing me to do my very best.

TABLE OF CONTENTS

LIST OF TABLES

LIST OF FIGURES

ABSTRACT

Estimation of age is an important component of the biological profile that forensic anthropologists construct in order to attain a positive identification of a deceased individual. This research is a proof of concept study for the use of x-ray diffraction (XRD) on a tooth sample to estimate age. Previous research (Meneghini et al. 2003; Hanschin and Stern 1992) has concluded that the crystallite size of bone will increase with increased age.

The feasibility of the use of teeth in XRD analysis was first tested using pig teeth (samples P1, P2, and P3). Another set of pig teeth (PC1, PC2, and PC3) were analyzed to determine if there were differences in tooth type for a single individual. Tooth samples were collected from individuals of known age in order to establish whether the crystallite size of hydroxylapatite changes with increased chronological age. All samples were cleaned and prepared using the same set of procedures. The resulting diffraction patterns from the XRD testing were analyzed using Jade 6 software to determine the full width half maximum (FWHM) for each of the samples. The crystallite size was then calculated using Scherrer's formula.

The first set of pig samples proved that it was possible to analyze teeth with XRD. The second set of samples demonstrated that there were crystallite size differences in the tooth types. The human teeth confirmed that there were differences in tooth type and presented evidence that there was a downward correlation between chronological age and crystallite size in teeth. Due to the rejection of the initial hypothesis, an alternative hypothesis was constructed stating that the crystallite size of the hydroxylapatite will decrease in teeth as age increases in an individual. Results of this research suggest the trend toward a decrease in crystallite size as an individual increases in age.

CHAPTER ONE: INTRODUCTION

Forensic anthropology is an important application of anthropological techniques in today's world. A combination of human osteology and criminal justice is used to construct a profile of a set of remains to aid law enforcement agencies. Due to the necessity of knowing the habits of human beings when reconstructing a forensic case, the holistic approach of anthropology plays an overt part in this process. According to Byers (2008), the five main objectives of a forensic anthropologist are to build a biological profile of the remains, identify trauma that is evident on bone, determine a postmortem interval, recover remains using archaeological techniques, and provide information to positively identify the deceased person.

The determination of age at death of a set of skeletal remains is an essential element of the biological profile that a forensic anthropologist assembles when evaluating a case. The ability to determine the age of a deceased individual from a single tooth using a technique that does not require a visual examination could be a valuable tool in a variety of forensic contexts. The examination of the mineral content of teeth could be employed as long as one tooth is present with the remains. It could also help to confirm age estimations made with other aging techniques; such as a multivariate approach could be important for reducing the amount of error in age assessment (Lovejoy et al. 1985). In addition to forensic situations, this technique could be used in an archaeological investigation to determine age-related demographic information for any archaeological site that contains human teeth.

This research is a proof of concept study on the viability of using X-ray powder diffraction (XRD) technique on teeth as a way of estimating age at death. The crystalline portion of teeth is called hydroxylapatite, or hydroxyapatite. This material can be analyzed with XRD to measure crystallite size (Wopenka and Pasteris 2005). Previous research on bone apatite has reported

trends toward increased crystallite size with increased age (Verdelis et al. 2007; Handschin and Stern 1992).

This research was designed to test the correlation between age and the crystallite size in the hydroxylapatite of teeth through a method of analysis with an X-ray diffractometer. Tooth samples were collected from individuals of known age in order to establish whether the crystallite size of hydroxylapatite changes with age. The hypothesis for this study states that the crystallite size of the hydroxylapatite found in teeth will increase with the age of an individual. This hypothesis can be accepted if the null hypothesis that the crystallite size of the apatite will have no correlation with age is rejected.

CHAPTER TWO: LITERATURE REVIEW

2.1 Importance of Age Estimation

A biological profile consists of an estimation of sex, ancestry, stature, and age. Forensic anthropologists can use features on the skull like eye orbit shape, nasal opening width, palatal shape, and metric analysis through a program such as FORDISC (Ousley and Jantz 2005) to determine possible ancestry (Bass 2005). The two regions that are the most useful for determining the sex of a skeleton are the head and pelvis. Features such as the ventral arc, subpubic angle, and size of the pelvic inlet in the pelvis and the prominence of the mastoid processes, supra-orbital ridge, and the mental eminence in the skull are a few of the ways to determine sex (White and Folkens 2005). Measurement of the long bones (i.e. femur, tibia, and humerus) with an osteometric board and application of those measurements to a formula based on sex and ancestry are common methods for determining living stature (Byers 2008). Many forensic anthropologists employ the use of dentition and epiphyseal closure in sub-adults and the auricular surface, pubic symphysis, and sternal rib ends in adults for estimation of age at death (Bass 2005). All of the current aging methods are based on the principle that the human skeleton undergoes specific and predictable changes throughout a person's lifetime. In those individuals who have not reached adulthood, examination of tooth eruption, development, and wear are the most accurate indicators of age. Once the wisdom teeth have completed development around the age of 21, the development status becomes obsolete and other techniques must be used.

Dentition is used in both subadults and adults to estimate age at the time of death. "Because of the regular formation and eruption times for teeth and because these elements are the remains found most commonly in forensic, archaeological, and paleoontological contexts, dental development is the most widely used technique for aging subadult remains" (White and Folkens 2005:364). The use of dentition in subadults is very well documented, but once all of the teeth

have erupted and the individual moves into adulthood, the analysis of rate and pattern of tooth wear becomes the only method of assigning age. Both of these methods can be affected by variations in individual populations, diet, heredity, and environment.

Current methods used to estimate age at death are associated with varying amounts of error and require that a panel of techniques be used to cross check estimations. A method based on XRD potentially could be used when the teeth are the only elements that are well preserved. Based on the past research conducted on bone and dentin apatite with the XRD, measuring the width of diffraction pattern peaks to approximate crystallite size could help to determine age at death if a change with age exists. A brief review of XRD fundamentals and their application to skeletal and dental research will provide background for the current study.

2.2 Fundamentals of XRD

XRD is a technique that can be used to analyze any crystalline material. A material is considered crystalline if its molecules or atoms are arranged in a regular manner in a three-dimensional space or crystal lattice (Hebbar 2007). This lattice structure is constructed of unit cells arranged in even rows and columns. Unit cells are the smallest repeating unit within the lattice. Figure 2.1 shows a small portion of a crystal lattice with a unit cell outlined in black. The size, shape, and orientation of adjacent unit cells determine the structure of the crystal. Many vary in degree of perfection giving rise to domains with different average crystallite sizes. The perpendicular distances (d) between the planes bounding the unit cell are unique and distinctive for each crystalline substance.

XRD is used to analyze powdered crystalline samples and single crystals. Hydroxylapatite in teeth is not arranged into large single crystals; therefore, the samples in this study need to be analyzed using the powdered crystalline method. All powdered crystalline samples contain thousands of individual crystals that are oriented in every possible direction (Glusker et al. 1994).

When an X-ray beam is produced by the XRD X-ray source, the X-ray hits the sample and diffracted radiation comes from the sample as shown in Figure 2.2 (Robinson et al. 2005). The beam is detected by the XRD at the angle of diffraction 2θ. The angle of this diffraction and d-values of the unit cell are related by the Bragg Reflection Analogy, $n\lambda = 2d \sin\theta$, where n is an integer determined by the order, λ is the wavelength, d is the spacing between planes in the lattice, and θ is the angle between the produced X-ray beam and resulting diffracted radiation (Hebbar 2007). A diffraction pattern produced from the diffracted X-rays collected by scanning 2θ will then contain multiple peaks representing the most heavily populated atomic planes in the unit cell. The peaks are then used to determine the full width at half maximum (FWHM) for the sample. FWHM is the measurement of the peak width (x_2-x_1) at half of the height of intensity (1/2 f_{max}) as shown by the bolded line in Figure 2.3.

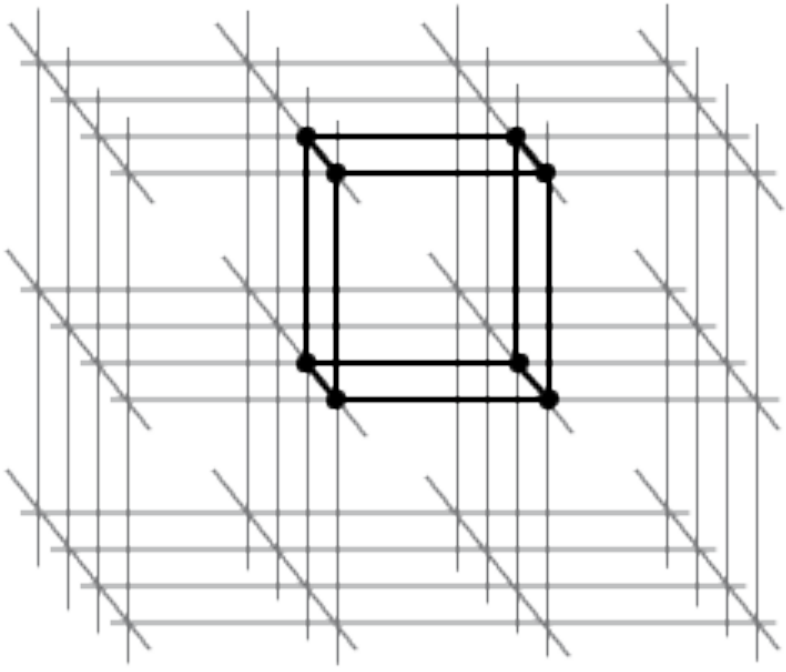

Figure 2.1 A Portion of a 3D Crystal Lattice with a Unit Cell in Heavy Outline. Adapted from Hebbar (2007).

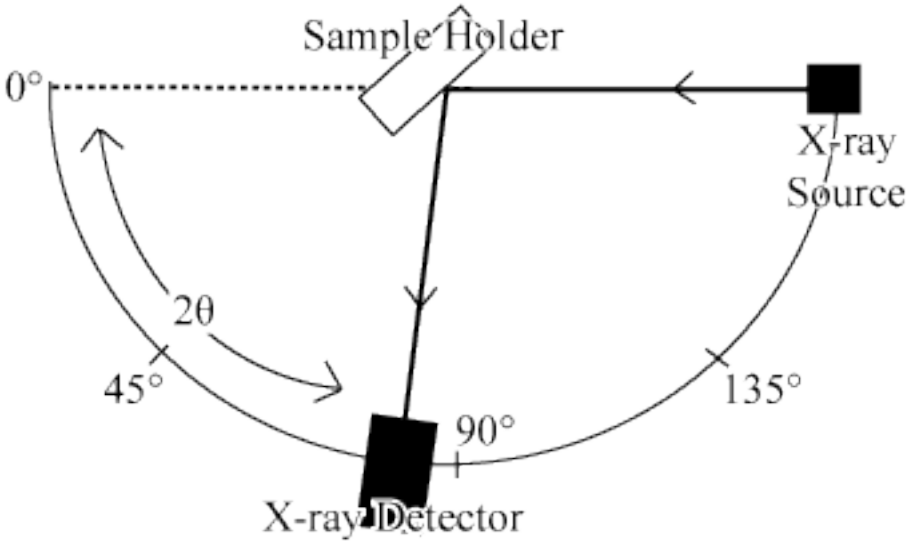

Figure 2.2 Schematic of Sample Analysis with an X-Ray Diffractometer. Adapted from Robinson et al. (2005).

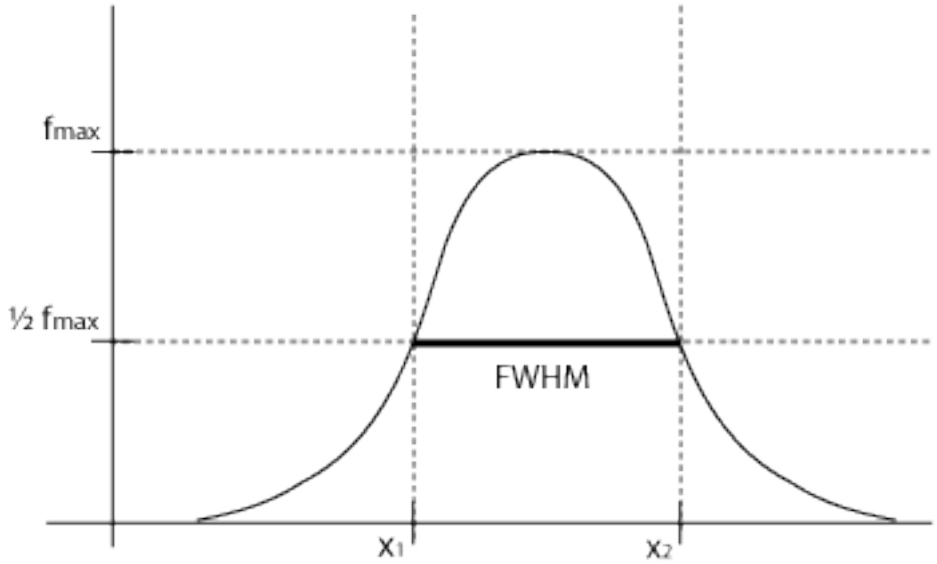

Figure 2.3 Full Width at Half Maximum of a Peak

2.3 Additional Methods: Hydroxylapatite and XRD

De Jong (1926) was the first to use wide-angle X-ray diffraction to analyze bone. His research established the fact that bone had an apatite-like crystal structure. Robinson and Watson (1955) established the connection between apatite crystallite size and age. Chatterji and Jeffery (1968) later expanded on this idea in their research into how the structure of bone changes with

age. This early research was conducted in order to establish how bone changes through the lifetime of mammals.

The crystalline materials making up bone and teeth belong to the apatite group. Bone and dentin apatite are most closely related to hydroxylapatite in both structure and composition (Wopenka and Pasteris 2005). Minerals of the apatite group exhibit a crystalline structure composed of $Ca_5(PO_4)_3(OH)$. XRD provides the basis for the qualitative and quantitative identification of the molecules present in crystalline hydroxylapatite powders (Robinson et al. 2005).

Since De Jong ascertained that the mineral portion of bone was composed of apatite, the consensus has been that bone apatite was identical to hydroxylapatite. Recent advancements in technology have shown that although bone apatite and hydroxylapatite are very closely related, they exhibit some important distinguishing characteristics. The slight size, structure, orientation, and compositional differences between these two types of crystals give them different properties. Mineral hydroxylapatite has a specific structure that exists only under limited environmental conditions. Bone apatite does not have a single uniform structure or composition. Biochemical activity makes the hydroxylapatite composition vary greatly, depending on cellular metabolism, age, diet, and diseases (Meneghini et al. 2003).

Bone apatite crystallites are in the nanometer range, while geological apatite is in the millimeter to centimeter range (Wopenka and Pasteri 2005). This size difference is very important to the function of both materials. The larger size of geological apatite gives it stability and a rigid structure, which makes it easily broken. The smaller size of the bone apatite still gives the bone structure, but also allows for bone remodeling and for the greater resistance to weight load that bone needs to endure. The increase in crystallite size is believed to be the cause for brittle bones in older individuals (Vetter et al. 1991). Crystal size increases by the addition of ions and by the

aggregation of crystals, a process called "second nucleation." In young bone, a composite of recently formed small crystals and mature large crystals can be found. This mixture of small and large crystals may represent the optimal situation for good resistance to load. The bone maturation process involves structural changes related to the composition of bioapatite (Meneghini et al. 2003). The bioapatite crystallites are initially small and elongated along the crystallographic c axis, and they grow as bone maturation proceeds; thus, in aging bone, the average crystal size increases. Bone becomes more brittle as one ages because of the greater number of large crystals and tends to fracture more easily (Augat and Schorlemmer 2006).

2.4 Crystallite Size

XRD is sensitive to changes in long-range atomic order in a crystalline material. XRD peaks become sharper and more intense, as the continuity of atomic planes and crystallite size increases (Wopenka and Pasteri 2005). As the crystallite size increases, the increase in length-scale of atomic planar continuity can be seen in the reduced FWHM of the diffraction peaks (Wopenka and Pasteri 2005:38). The diffraction peaks from fetal bone samples are broader than those of adult bone, indicating that the crystallites in the younger bone are smaller than in adult bones (Meneghini et al. 2003). Peak widths may be converted directly to average crystallite size with an expression developed by Scherrer (Meier 2004).

Two approaches for implementing Scherrer's formula in hydroxylapatite ($<L>_{vol} = K\lambda / \beta_{1/2} \cos \theta_{\beta}$) involve the use of a single peak and a combination of several peaks. For the purpose of this study, peaks will be identified by either the (hkl) designation for the planes in the unit cell or by their d-values (see Figure 2.3). The (hkl) designation or Miller indices are the symbolic illustration of atomic planes in a crystal lattice (Hebbar 2007). Hanschin and Stern (1992) observed that the region from 30° to 35° 2θ in the pattern that contains the (211), (112), (300), and (202) peaks was so heavily overlapped that the data could not be assessed accurately (see Figure

2.4 for labeled peak locations). The same study identified peak (002) as the best candidate for analysis because it was isolated and not affected by peak overlap. Several studies have also used this single peak method (Rusu et al. 2005; Thamaraiselvi et al. 2006; Ye et al. 2008), while others have studied the multiple peak method (Sidaway 1979; Chang et al. 1998; Chang et al. 1999) by performing a peak decomposition of the overlapping peaks.

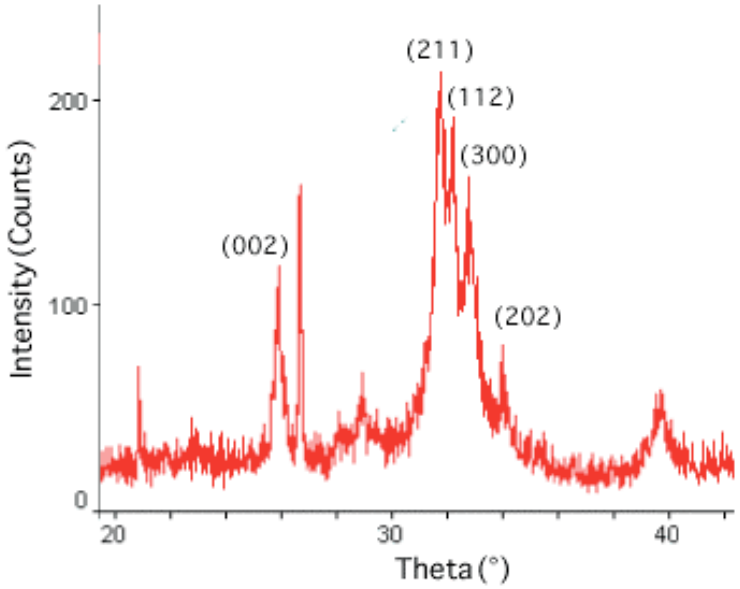

Figure 2.4 Example of a Diffraction Pattern of Sample P1 with Peaks (002), (211), (112), and (300) labeled.

2.5 Tooth Components

Teeth are composed of three components: dentin, enamel, and cementum. Dentin is the internal component of teeth that is coated with enamel at the crown and cementum at the root (Hillson 1996). Teeth undergo similar processes as non-dental bone but have a few characteristics that make them more appropriate for this study. Verdelis et al. (2007) showed that, unlike bone, the dentin and cementum portions of teeth do not undergo remodeling and are good candidates for analyzing age-related changes in teeth. Bone remodeling is the resorption of old bone and the

addition of new bone that occurs throughout an individual's lifetime in response to trauma, pathology, and age. Although no remodeling of teeth occurs, the deposition and formation of secondary and tertiary dentin may contribute to the age-related changes (Kuttler 1959). Trautz (1955:696) said, "Dental enamel has been chiefly used [in X-ray diffraction studies] since its apatite is more highly crystalline than apatite of bone." Dentin is composed of crystals that are of similar size to the crystals found in non-dental bone, but the enamel crystals are about ten times the size of dentin crystals (Kirkham et al. 1998).

2.6 Tooth Development

Teeth begin to develop in the mouth long before birth. The enamel forms as a progression of layers on the outside of the forming tooth and dentin is deposited on the inferior portion of the enamel layers (Hillson 1996). Each type of tooth begins development at different times in a person's life, and each tooth has a different growth rate due to their variable size and shape. A set of deciduous teeth or "milk" teeth develop in infants and are subsequently replaced by a permanent set of teeth closer to adulthood. As they age, children lose their deciduous teeth at predictable times. Most children have lost all of their deciduous teeth by age 12 or 13 years (Woelfel and Scheid 2003:3). Each deciduous tooth is lost in a process that involves the development of a permanent tooth that stimulates the dissolution of the root of the deciduous tooth. The development of the permanent teeth occurs in stages and the deciduous teeth are lost gradually over time. The crowns of the permanent teeth develop under the roots of the deciduous teeth and push to the surface when the development of the tooth is complete. This natural progression results in permanent teeth that are "older" than other permanent teeth in the same mouth. Carlos and Gittelsohn (1965) conducted the first comprehensive study on eruption patterns of permanent teeth in contemporary populations. The data collected resulted in a timeline for the eruption of each tooth for both male and female children (Table 2.1).

Table 2.1 Tooth Types and Positions Ranked for First Eruption (1) to Last Eruption (14). Adapted from Carlos and Gittelsohn (1965).

Rank	Tooth Type and Position	Age at Eruption
1	Mandibular Central Incisors	6.3-6.6 years
2	Mandibular First Molars	6.5-6.8 years
3	Maxillary First Molar	6.6-6.8 years
4	Maxillary Central Incisors	7.3-7.6 years
5	Mandibular Lateral Incisors	7.4-7.7 years
6	Maxillary Lateral Incisors	8.3-8.7 years
7	Mandibular Canines	9.9-10.8 years
8	Maxillary First Premolars	10.3-10.7 years
9	Mandibular First Premolars	10.4-10.7 years
10	Maxillary Second Premolars	11.0-11.2 years
11	Mandibular Second Premolars	11.0-11.3 years
12	Maxillary Canines	11.0-11.6 years
13	Mandibular Second Molars	11.2-11.9 years
14	Maxillary Second Molars	12.1-12.2 years

2.7 Pig Proxy

Pigs have been used in forensic research for years due to the numerous similarities that they hold with humans. "The domestic pig appears to be the most acceptable animal as a model, and it has been used frequently in recent decomposition studies" (Catts and Goff 1992:261). In addition to their physiological and developmental similarities to humans, pigs are abundant and easily obtained for study. This research contains samples that are both domestic pig (P1 and P2) and wild boar (P3).

Very few differences exist between the domestic pig and the wild boar. Pig premolars are sometimes mistaken for human molars in forensic contexts because of the similarity in tooth shape. This resemblance stems from the similar omnivorous diet that requires a design for both plant material and meat (Dupras et al. 2005). Matschke (1967) performed a study on the tooth

eruption patterns of wild boars and domestic pigs. The study concluded that the teeth in both groups would erupt in close correlation to one another.

Magnell and Carter (2007) noted in their study of wild boars and wild boar/domestic pig hybrids that there is little difference in structure or size between these two groups. They stated that this comparison could not be extended to non-hybrid domestic pigs because of the variance of diet. Wild boars go through periods of malnutrition that result in lines of enamel hypoplasia. Enamel hypoplasia is a visible area of arrested development within the crystalline structure of the enamel. Since the enamel is not progressing through normal stages of growth, any age determination based on growth will be imperfect. Most domesticated pigs are fed regularly and do not have lines of enamel hypoplasia due to their abundant diet. The dietary, morphological, and developmental similarities between pigs and humans make them a suitable proxy for human samples in the initial stages of this study.

2.8 Current Research in Hydroxylapatite and XRD

Current XRD research in the forensic sciences ranges from analysis of cremains to the development of a technique of identifying species from bone samples. Bodkin and Mies (2008) used the method of analyzing bone with XRD to distinguish between bone and concrete. Their research was conducted in response to the events that occurred at the Tri-State Crematory. Evidence showed that at least some of the cremains returned to clients were actually a mixture of concrete and bone. Bodkin and Mies were able to use this method to test known human cremains, animal cremains, and concrete against the contents of the cremains returned to the families. Beckett and Rogers (2008) of the Cranfield Forensic Institute at the Cranfield University in the United Kingdom have been using a method of pyrolysis and XRD of bone to identify species. They have shown that the d-values and intensities of certain hydroxylapatite peaks are different between animal species.

XRD analysis of hydroxylapatite has applications outside of forensics. Hydroxylapatite is being used to coat titanium surgical implants to discourage rejection by the bone. Several studies have been done on the effectiveness of this coating technique have been performed using XRD analysis (Jansen et al. 1991; McPherson et al. 1995). The use of various biological apatites (i.e. hydroxylapatite, fluorapatite, fluorhydroxyapatite) to coat dental implants has become a common practice. Gineste et al. (1999) and Baltag et al. (2000) studied the integration of these coatings with the surrounding bone using XRD.

2.9 Research Plan

Problems still remain with the studies that have been conducted and the methods in which forensic anthropologists estimate age at death. As a result, this research focuses on the use of hydroxylapatite crystallite size in teeth to determine age. Samples of both pig and human teeth were prepared for powder diffraction analysis to verify the viability of an XRD technique for age estimation. The methodology for this study is presented in Chapter 3.

CHAPTER THREE: MATERIALS AND METHODS

Tooth samples were extracted and collected from four pigs and ten human individuals for a total of 16 samples. Three samples were collected from three separate pigs to determine whether the XRD techniques could detect variation among individuals. These samples came from one wild pig (*Sus scrofa*) and two domestic pigs. Three of the samples were collected for the study of intra-individual variation from one domestic pig (*Sus domesticus*). The remaining ten samples were collected from ten human individuals of varying ages for the study of variation of age within humans.

The samples were compared on the basis of age, species, tooth type, and position of tooth in the mouth. The first test conducted on samples P1, P2, and P3 was to determine if the hydroxylapatite in teeth would yield peak intensities that would allow for crystallite size analysis. The second test was to compare the composition and crystallite size of P1, P2, and P3. The third test looked at the crystallite size and compositional differences of PC1, PC2, and PC3 to determine the amount of variation found across the tooth types in a single individual. The fourth test compared samples H1 through H10 for a crystallite size and age correlation. The ages were evaluated and compared by grouping the samples into sets based on tooth number (i.e. #20, #21, #13, and #11). These sets were evaluated separately and then together as one sample population.

3.1 Sample

Three pig teeth were collected from one pig of known age and sex. "Pig C" was involved in the thesis research of Ms. Lauren Pharr during the summer and fall of 2008. An incisor, a premolar, and a molar were extracted from the completely skeletonized mandible. The pig was still undergoing the effects of decomposition and the samples were thoroughly washed with soap and water to remove organic matter.

Teeth from three other pigs were taken from the Louisiana State University Forensic Anthropology and Computer Enhancement Services (FACES) Laboratory faunal comparative collection. One mandibular molar was extracted from each of the specimens. No age or sex information was available about the pigs because they were donations or found specimens. Analyzing tooth eruption patterns, epiphyseal closure of the long bones, and overall size of the specimen gave the approximate age of each pig. The two domestic pigs had skulls that appeared to be the same size with the same amount of tooth eruption and were estimated to be juveniles nearing adulthood. The wild pig skull was significantly larger than the domestic pigs, but tooth eruption pattern was similar to that of the juvenile domestic pigs.

All ten human samples were obtained from the donated collection at the LSU FACES Laboratory. Individual samples were chosen from the collection to encompass as wide an age range as possible. The ages of the individuals ranged from 17 years old to 64 years old. Most of the samples are of mandibular left first premolars, but other teeth were collected when that tooth was unavailable (Table 3.1). The teeth were selected by laboratory personnel and placed in coded envelopes for this researcher's blind study.

3.2 Sample Preparation

After collection, each tooth was washed with deionized water to remove any residual dirt and organic matter from the surface. Some of the human samples had remnants of Elmer's glue on the root from being secured previously in the socket. The samples from Pig C needed to be washed several times to remove decaying matter from the exterior. Once clean, the samples were photographed and weighed (Table 3.2).

Table 3.1 Name, Genus, Species, Age, Sex, and Tooth Type for the Study Sample.

Name	Genus species	Age	Sex	Tooth Type
P1	*Sus domesticus*	Juvenile	Unknown	Mandibular Right Second Molar
P2	*Sus domesticus*	Juvenile	Unknown	Mandibular Right First Molar
P3	*Sus scrofa*	Juvenile	Unknown	Mandibular Right First Molar
PC1	*Sus domesticus*	1 Year	Male	Mandibular Right First Molar
PC2	*Sus domesticus*	1 Year	Male	Mandibular Left First Premolar
PC3	*Sus domesticus*	1 Year	Male	Mandibular Central Incisor
H1	*Homo sapiens*	Late 40's	Male	Mandibular Left Second Premolar
H2	*Homo sapiens*	43 Years	Female	Mandibular Left Second Premolar
H3	*Homo sapiens*	64 Years	Male	Mandibular Left Second Premolar
H4	*Homo sapiens*	20 Years	Female	Mandibular Left Second Premolar
H5	*Homo sapiens*	53 Years	Male	Maxillary Left Second Premolar
H6	*Homo sapiens*	17 Years	Female	Mandibular Left First Premolar
H7	*Homo sapiens*	24 Years	Male	Mandibular Left First Premolar
H8	*Homo sapiens*	25 Years	Male	Mandibular Left First Premolar
H9	*Homo sapiens*	21 Years	Male	Mandibular Left First Premolar
H10	*Homo sapiens*	36 Years	Female	Maxillary Left Canine

Table 3.2 Condition and Weight of Samples.

Name	Tooth Number	Initial Weight	Micronized Weight	Comments
P1	n/a	1.2g	1.0g	Skeletonized pig
P2	n/a	1.3g	1.1g	Skeletonized pig
P3	n/a	1.6g	1.5g	Skeletonized pig
PC1	n/a	1.2g	1.1g	Pig in active decomposition
PC2	n/a	1.1g	.9g	Pig in active decomposition
PC3	n/a	.7	.6g	Pig in active decomposition
H1	20	1.3g	1.1g	None
H2	20	1.4g	1.2g	Glue on root
H3	20	1.1g	.9g	None
H4	20	.9g	.7g	White crown, dark root, glue on root
H5	13	1.3g	1.2g	Mesial carious lesion, CEJ calculus
H6	21	.8g	.8g	Glue on root
H7	21	.9g	.8g	Excess dirt, dark brown stains
H8	21	1.1g	1.0g	Crown split buccal to lingual
H9	21	1.1g	1.0g	Excess dirt
H10	11	.9g	.7g	Severe attrition, excess dirt

3.2.1 Micronization

Each sample was ground into a coarse powder using a mortar and pestle or a percussion mortar. The use of the mortar and pestle worked best for the cementum and dentin portion of the tooth. Due to the dense mineralization of enamel, parts of the tooth required a percussion mortar to break the sample into smaller and more manageable portions. Special care was taken in cleaning the mortar and pestle, utensils, and surfaces used during preparation to insure that no cross contamination occurred.

For XRD analysis, the coarse powders were reduced to an average diameter of 5 μm in a McCrone micronizer. The sample was poured between the corundum elements of the milling cylinder. Care was taken not to pour the sample on top of the milling elements so that the entire sample was milled in a uniform manner. With the use of a syringe, 10 mL of ethanol was added to the cylinder and it was capped. The mill was run for five minutes. An additional 10 mL of ethanol was added to the cylinder and the contents were poured into a large plastic test tube. To remove all remaining sample from the cylinder, 10 mL of ethanol was added to the cylinder. It was gently shaken and poured into the test tube. This was repeated until the solution was clear and free of any sample.

The test tubes were placed into a centrifuge for 20 minutes to remove excess ethanol. Each test tube was then transferred to a low temperature (60°C) oven to dry overnight. The micronized samples were then homogenized using a mortar and pestle before being placed into glass vials for storage until they were loaded into the XRD sample holders.

3.2.2 Sample Mounting

Samples were loaded into individual aluminum sample holders using the side-drift method that involved clamping the holder to a plastic sample loader. A small amount of sample was placed in the opening of the sample holder using a spatula. The assembly was then tapped to

allow the sample to pack into the well in the center of the sample holder. Once the sample looked evenly packed, more sample was added to the loader and the process was repeated until the sample filled the entire well. The loader was removed and the sample in the holder was tested for proper packing by tilting the holder to a vertical position. If the sample stayed packed and did not shift, the sample was loaded properly. Each sample holder was labeled (i.e., Pig 1, Pig 2, Pig 3) in pencil. Each sample was run in a Siemens D5000 diffractometer at 40 kV and 30 mA according to the protocols in Table 3.3.

Table 3.3 XRD Protocol for Each Run of All Samples

Sample	Angle Range	Step Size	Time Per Step
P1 (Run #1)	2 deg - 70 deg	0.02 deg	2.0 sec
P2 (Run #1)	2 deg - 70 deg	0.02 deg	2.0 sec
P3 (Run #1)	2 deg - 70 deg	0.02 deg	2.0 sec
P1 (Run #2)	2 deg - 70 deg	0.02 deg	4.0 sec
P2 (Run #2)	2 deg - 70 deg	0.02 deg	4.0 sec
P3 (Run #2)	2 deg - 70 deg	0.02 deg	4.0 sec
PC1	2 deg - 70 deg	0.02 deg	8.0 sec
PC2	2 deg - 70 deg	0.02 deg	8.0 sec
PC3	2 deg - 70 deg	0.02 deg	8.0 sec
H1	10 deg -70 deg	0.02 deg	8.0 sec
H2 (Run #1)	10 deg -70 deg	0.02 deg	8.0 sec
H2 (Run #2)	10 deg -70 deg	0.02 deg	8.0 sec
H3	10 deg -70 deg	0.02 deg	8.0 sec
H4	10 deg -70 deg	0.02 deg	8.0 sec
H5	10 deg -70 deg	0.02 deg	8.0 sec
H6	10 deg -70 deg	0.02 deg	8.0 sec
H7	10 deg -70 deg	0.02 deg	8.0 sec
H8	10 deg -70 deg	0.02 deg	8.0 sec
H9	10 deg -70 deg	0.02 deg	8.0 sec
H10	10 deg -70 deg	0.02 deg	8.0 sec

3.3 Qualitative Analysis

The diffraction patterns for each sample were analyzed using the Jade 6 software program (Materials Data 2001). The 2-theta, d-value, intensity, and FWHM of all peaks were calculated by the program and tabulated as a d/I file. The identity of the hydroxylapatite and other minerals was determined with the search/match Jade routine. Peaks identified in sample H2 are shown by the dashed lines in Figure 3.1A.

3.3.1 Identification of Compounds

Jade generated a list of crystalline compounds that were "best" statistical matches to the peaks illustrated below in Figure 3.1. The list of potential matches was narrowed down using the position and intensity of each peak. Although the d-values did not match exactly, a match could still be made by statistically comparing all of the d-value shifts. The program established that hydroxylapatite [$Ca_5(PO_4)_3(OH)$] and quartz (SiO_2) were present in most samples. Figure 3.1 and Table 3.3 show an example of the peak identification output produced by the Jade software. Figure 3.1, B and C are representations of peak positions associated with hydroxylapatite and quartz reference data files, respectively. The correlation with peaks in 3.1A provides a visual check on the identification technique. The d-values for all peaks in the sample pattern are listed in Table 3.3 with their identity and hkl planes indicated. The peaks of interest for this study are highlighted in light gray in Table 3.4.

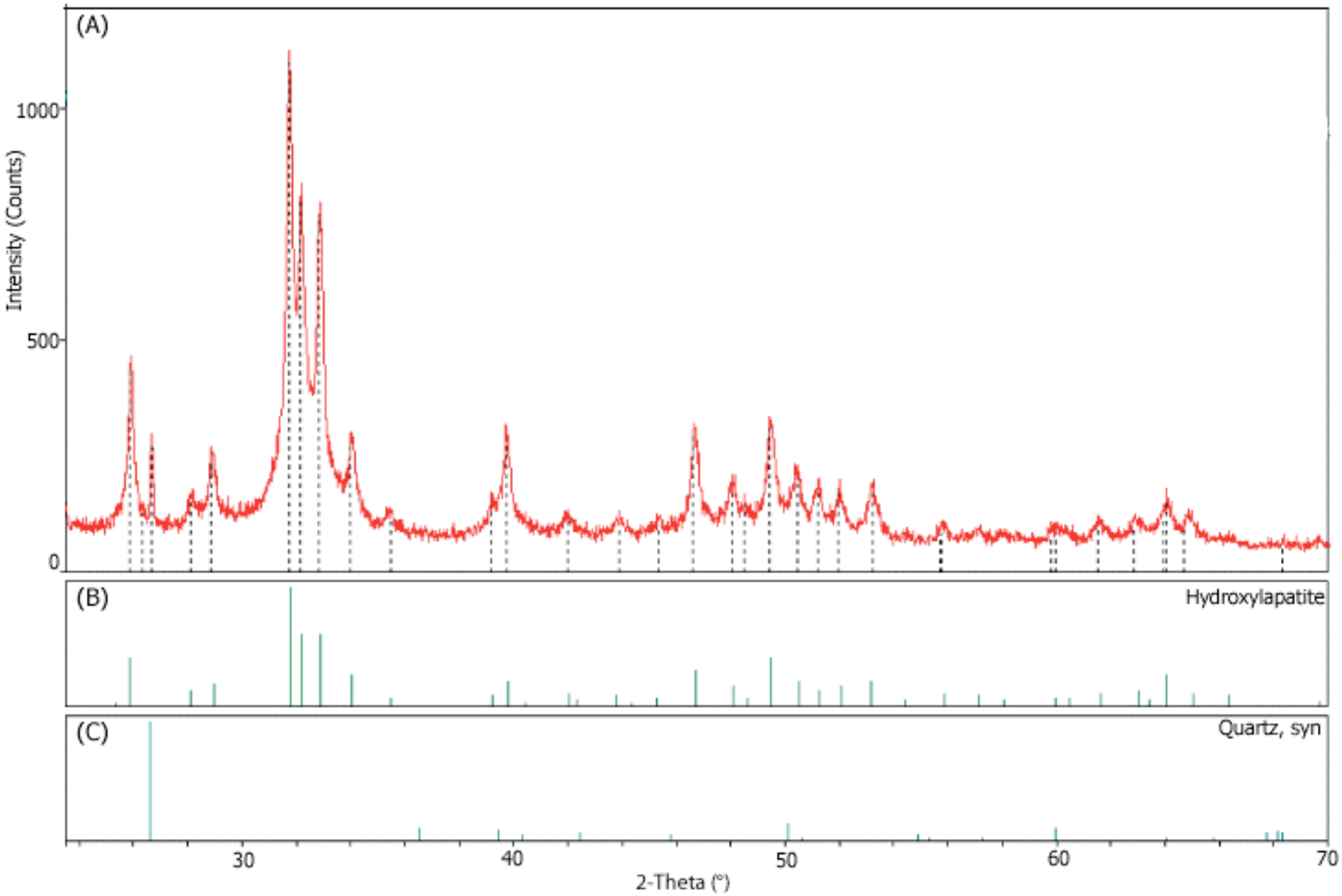

Figure 3.1 Peak Identification with Hydroxylapatite (B) and Quartz (C) Overlays Under the Diffraction Pattern of Sample H2 (A).

Table 3.4 Peak ID Report Showing 2-Theta, d-values for the Sample and the Identified Mineral with (h k l) Designations for the Diffraction Pattern in Figure 3.1.

2-Theta	d(A)	Phase ID	2-Theta	d(A)	(h k l)
10.443	8.4639				
10.764	8.2121	Hydroxylapatite, syn	10.82	8.17	(1 0 0)
16.838	5.2612	Hydroxylapatite, syn	16.841	5.26	(1 0 1)
20.875	4.2518	Quartz, syn	20.859	4.255	(1 0 0)
21.756	4.0816	Hydroxylapatite, syn	21.819	4.07	(2 0 0)
22.838	3.8906	Hydroxylapatite, syn	22.902	3.88	(1 1 1)
25.881	3.4397	Hydroxylapatite, syn	25.879	3.44	(0 0 2)
26.318	3.3835				
26.648	3.3424	Quartz, syn	26.639	3.3435	(1 0 1)
28.139	3.1686	Hydroxylapatite, syn	28.126	3.17	(1 0 2)
28.864	3.0906	Hydroxylapatite, syn	28.966	3.08	(2 1 0)
31.721	2.8185	Hydroxylapatite, syn	31.773	2.814	(2 1 1)
32.16	2.781	Hydroxylapatite, syn	32.196	2.778	(1 1 2)
32.859	2.7234	Hydroxylapatite, syn	32.902	2.72	(3 0 0)
33.983	2.6359	Hydroxylapatite, syn	34.048	2.631	(2 0 2)
35.464	2.5291	Hydroxylapatite, syn	35.48	2.528	(3 0 1)
39.175	2.2976	Hydroxylapatite, syn	39.204	2.296	(2 1 2)
39.739	2.2664	Hydroxylapatite, syn	39.818	2.262	(3 1 0)
41.978	2.1505	Hydroxylapatite, syn	42.029	2.148	(3 1 1)
43.873	2.0619	Hydroxylapatite, syn	43.804	2.065	(1 1 3)
45.343	1.9984	Hydroxylapatite, syn	45.305	2	(2 0 3)
46.621	1.9466	Hydroxylapatite, syn	46.711	1.943	(2 2 2)
48.019	1.8931	Hydroxylapatite, syn	48.103	1.89	(3 1 2)
48.497	1.8756	Hydroxylapatite, syn	48.623	1.871	(3 2 0)
49.423	1.8426	Hydroxylapatite, syn	49.468	1.841	(2 1 3)
50.438	1.8078	Hydroxylapatite, syn	50.493	1.806	(3 2 1)
51.217	1.7822	Hydroxylapatite, syn	51.283	1.78	(4 1 0)
51.962	1.7583	Hydroxylapatite, syn	52.1	1.754	(4 0 2)
53.235	1.7192	Hydroxylapatite, syn	53.143	1.722	(0 0 4)
55.703	1.6488				
55.772	1.6469	Hydroxylapatite, syn	55.879	1.644	(3 2 2)
59.783	1.5456	Hydroxylapatite, syn	59.938	1.542	(4 2 0)
59.996	1.5407	Quartz, syn	59.958	1.5415	(2 1 1)
61.506	1.5064	Hydroxylapatite, syn	61.66	1.503	(2 1 4)
62.872	1.4769	Hydroxylapatite, syn	63.011	1.474	(5 0 2)
63.92	1.4552				
64.041	1.4527	Quartz, syn	64.034	1.4529	(1 1 3)
64.707	1.4394				
68.321	1.3718	Quartz, syn	68.316	1.3719	(3 0 1)

3.3.2 Peak Decomposition

Isolated peaks that have no interference from surrounding peaks were ready for analysis, but overlapping peaks were separated to resolve individual peak parameters. Figure 3.2 shows the decomposition results for (211), (112), and (300) peaks for the diffraction pattern of sample H7.

The three colored peaks that appear in Figure 3.2 are representations of how the shape and size of the peaks would have appeared had there not been interference with the neighboring peaks. The solid vertical lines denote the original d-values that were assigned to the pattern before the decomposition and the dashed vertical lines are the adjusted d-values as a result of the decomposition. These resolved peaks also produced values for the FWHM that were used in determining crystallite size.

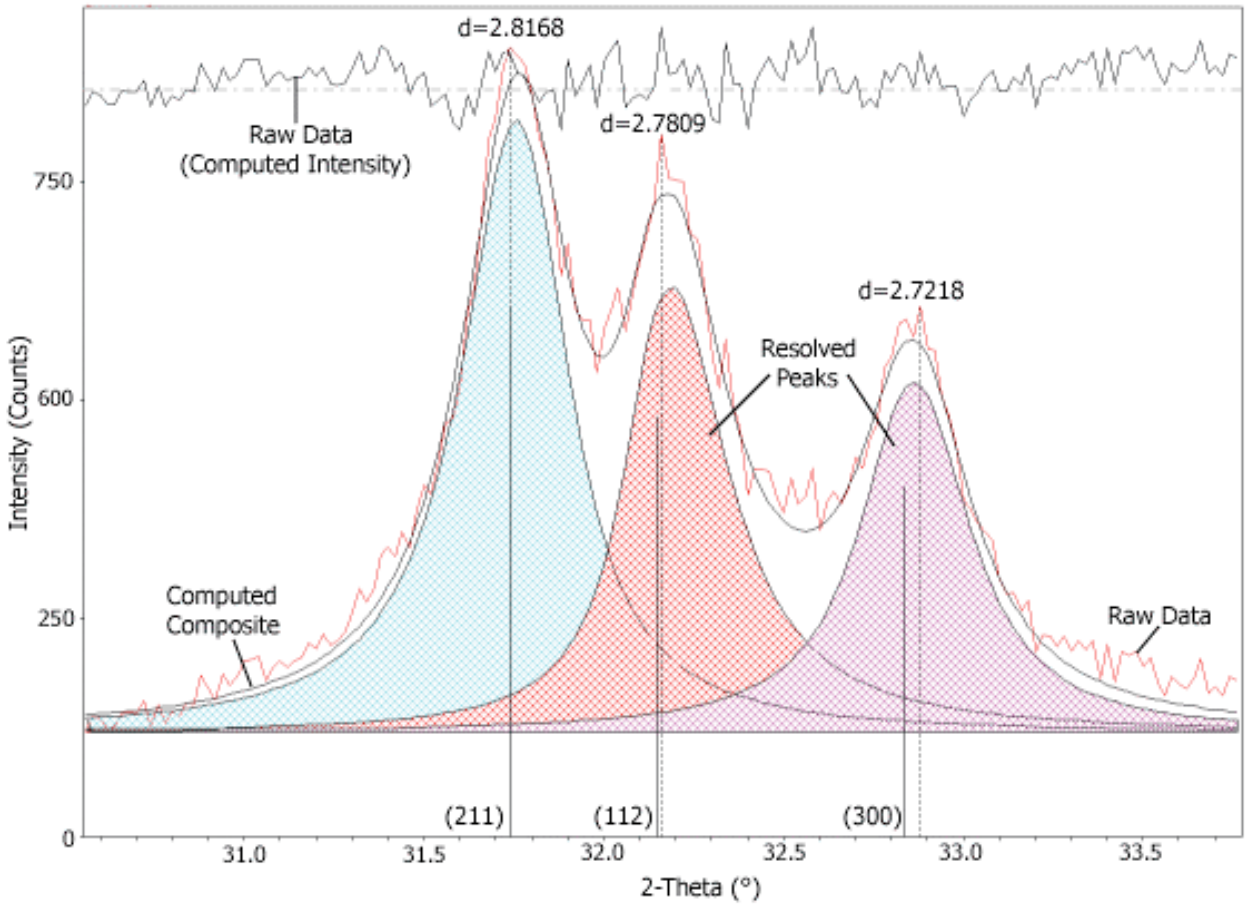

Figure 3.2 Peak Decomposition of (211), (112), and (300) Peak Grouping for H7. Intensity Scale Shown the Top. Hatched Areas Indicate Resolved Peaks. Vertical Dashed Lines through the Peaks are Original d-values and Solid Vertical Lines are the Resolved Peak d-values (Labeled).

3.3.3 Crystallite Size

Scherrer's formula was used to determine crystallite size from the analyzed peaks. This formula involves a constant (K), the source wavelength (λ), the FWHM ($\beta_{1/2}$), and the position of

the peak (θ_β) to determine the crystallite size for a particular peak. Scherrer's formula for a single peak is expressed as:

$$<L>_{vol} = K\lambda / \beta_{1/2} \cos \theta_\beta \quad (3.1)$$

where by $<L>_{vol}$ is the crystallite size. For the multiple peak method, a variation of Scherrer's forumula was employed. Each individual peak was analyzed for crystallite size and the average crystallite size for the three peak set for each tooth was obtained.

For both the single peak and multiple peak methods of comparing crystallite size in samples, each peak was individually analyzed using this formula. The single peak method allowed for each calculation for individual peaks to be compared with the same peak in another sample. For this research, peaks (002) and (310) were independently compared across all human samples to test the single peak method. The multiple peak method required two or more peaks to be analyzed and averaged. Peaks (211), (112), and (300) were used together to test the multiple peak method. In addition to their use in the multiple peak method, peaks (211), (112), and (300) were also evaluated individually and tested with the single peak method. This last test was to assess the effectiveness of peak decomposition on the amount of interference that peak overlap had on this group of peaks.

The data were compiled using three separate analyses for each tooth sample. PC1, PC2, PC3, H1, and H3 through H10 were replicated in the Jade software three times with no additional reanalysis using the XRD. Samples P1, P2, P3, and H2 were replicated twice using the Jade software and once by performing a second analysis with the XRD. The sample that was packed into the sample holder for the initial analysis was homogenized with the remaining powder from that sample and repacked into the sample holder for a second run.

CHAPTER FOUR: RESULTS

4.1 Tooth Composition

Results for samples P1, P2, and P3 confirmed that hydroxylapatite appeared as expected but there were also unanticipated quartz peaks. All of the remaining samples also contained hydroxylapatite and quartz. Quartz and hydroxylapatite relative intensities varied from sample to sample, indicating changes in the relative abundance of the two minerals.

4.2 Pig Tooth Analysis

The pig tooth samples that were used as a proxy for human teeth were valuable in determining the viability of this study. The application of peak decomposition was first used on samples P1, P2, P3, PC1, PC2, and PC3 for which it was determined that it was possible to isolate peaks (211), (112), and (300) for all samples. Peak (202) that is found in the region of 33.5° to 34.5° 2θ had to be removed from some of the decompositions due to poor intensity. Jade would only identify this peak in half of the samples because of its small size and lack of definition. Removal was done in all of the patterns where it was identified to maintain uniformity across the samples. An age comparison was not conducted on the pig samples because not all of the ages were known.

Crystallite size data of the (002) peaks for the three individual pig teeth (P1, P2, and P3) are illustrated in Figure 4.1. The multiple peak method was not employed on any of the pig data because peaks (211), (112), and (300) overlapped to the point that replication of the peak decomposition was not possible, which rendered these peaks unsuitable for analysis. Samples P1 and P2 show very little statistical difference at the 5% level (P=0.61) with a mean crystallite size difference of 0.8 nm. The crystallite sizes for P2 and P3 are significantly different at the 5% level (P=0.039) and demonstrate a 3.4 nm difference in mean crystallite size.

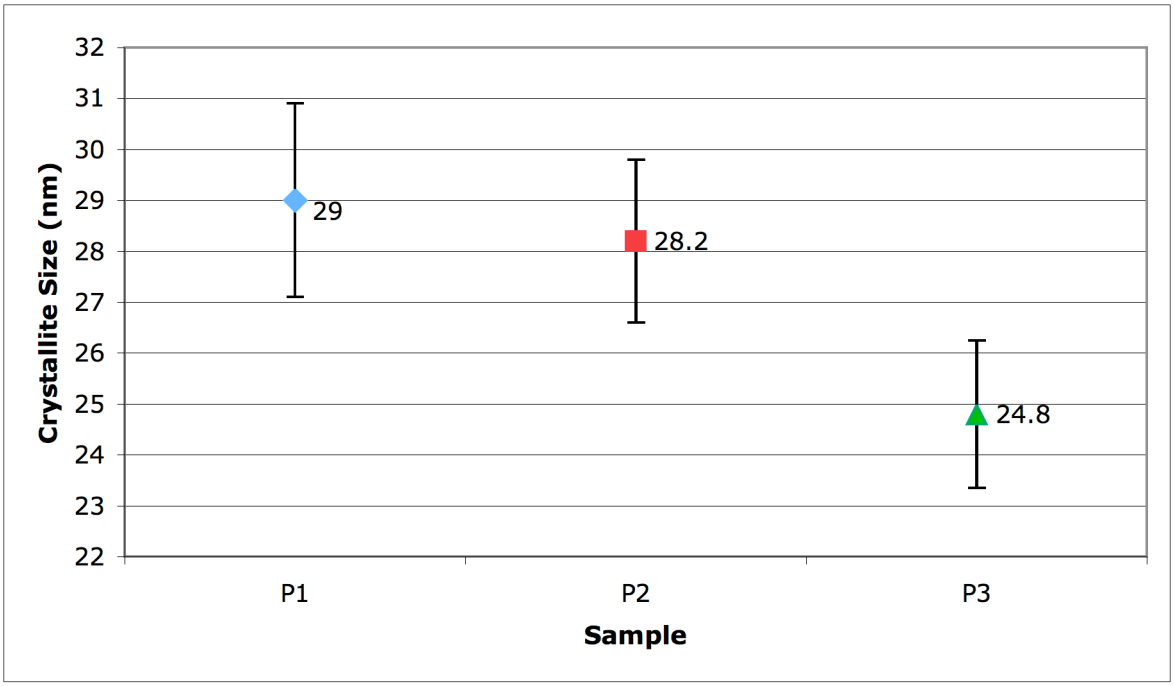

Figure 4.1 Graph Showing the Relationship Between Crystallite Size and the Teeth from Three Individual Pigs (P1, P2, and P3) Using the Single Peak Method (002).

4.2.1 Tooth Types

The three tooth samples collected from Pig C were compared to determine variation among tooth types for one individual. Figure 4.2 shows that the three types of teeth tested do demonstrate differences in crystallite size. Although there is an observable difference in Figure 4.2, the difference in crystallite size for the central incisor (triangle) and first premolar (square) are not statistically significant at the 5% level (P=0.14). Samples PC1 and PC2 show considerable similarity (P=0.9) with a mean crystallite size difference of 0.3 nm.

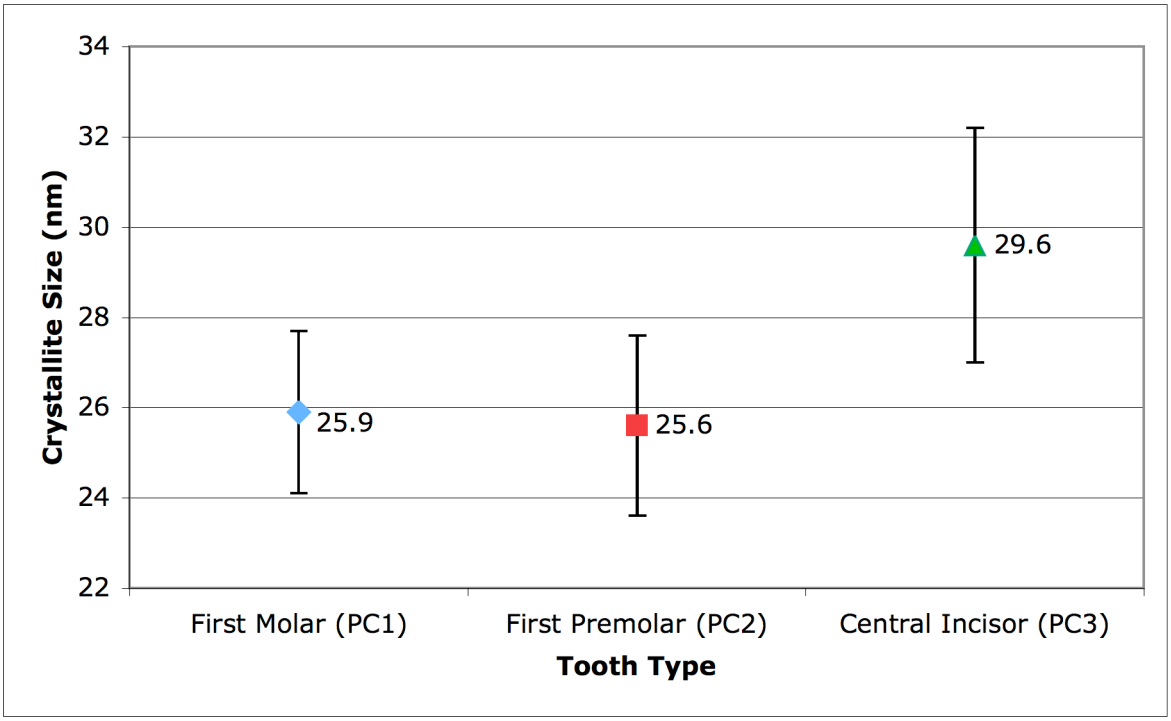

Figure 4.2 Graph Showing the Relationship Between Tooth Type and Crystallite Size for Tooth from One Pig Using the Single Peak Method (002).

4.3 Human Tooth Age Assessment

The human sample analyses were completed in two stages. Samples H1, H2, and H3 were the first to be analyzed with the XRD and evaluated with the Jade software. Samples H4 through H10 were analyzed in a second run of the instrument. H2 was rerun in this second step to compare any preparation or instrumental differences among runs.

4.3.1 Overall Age Comparison

Data from four different single peak analyses and one multiple peak determination were used in this analysis. The resulting data are tabulated in the Appendix and illustrated in Figures 4.3 to 4.10.

For the (002) peak, there was a general progression toward a smaller size with increased age based on the negative slope (-0.1309) in the linear regression formula (Figure 4.3). Samples H10 (36 years old), and H1 (48 years old) were the most anomalous of the data because the error

does not approach the linear regression line. The crystallite sizes for these samples resulted in figures that were lower than the other samples for this peak. Peaks H3 through H9 fell within the 40.96 to 35.80 nanometer (nm) range for crystallite size and demonstrated a downward progression based on age. The remaining peaks were in the 35.65 to 33.06 nm range and did not have any trend that correlated with age. The fit of the data for this line was R^2=0.5369. A logarithmic trend line was also applied to the data for the (002) peaks as illustrated in Figure 4.4. This regression also displays a negative slope (-1.9264) and has a better fit of the data (R^2=0.6614).

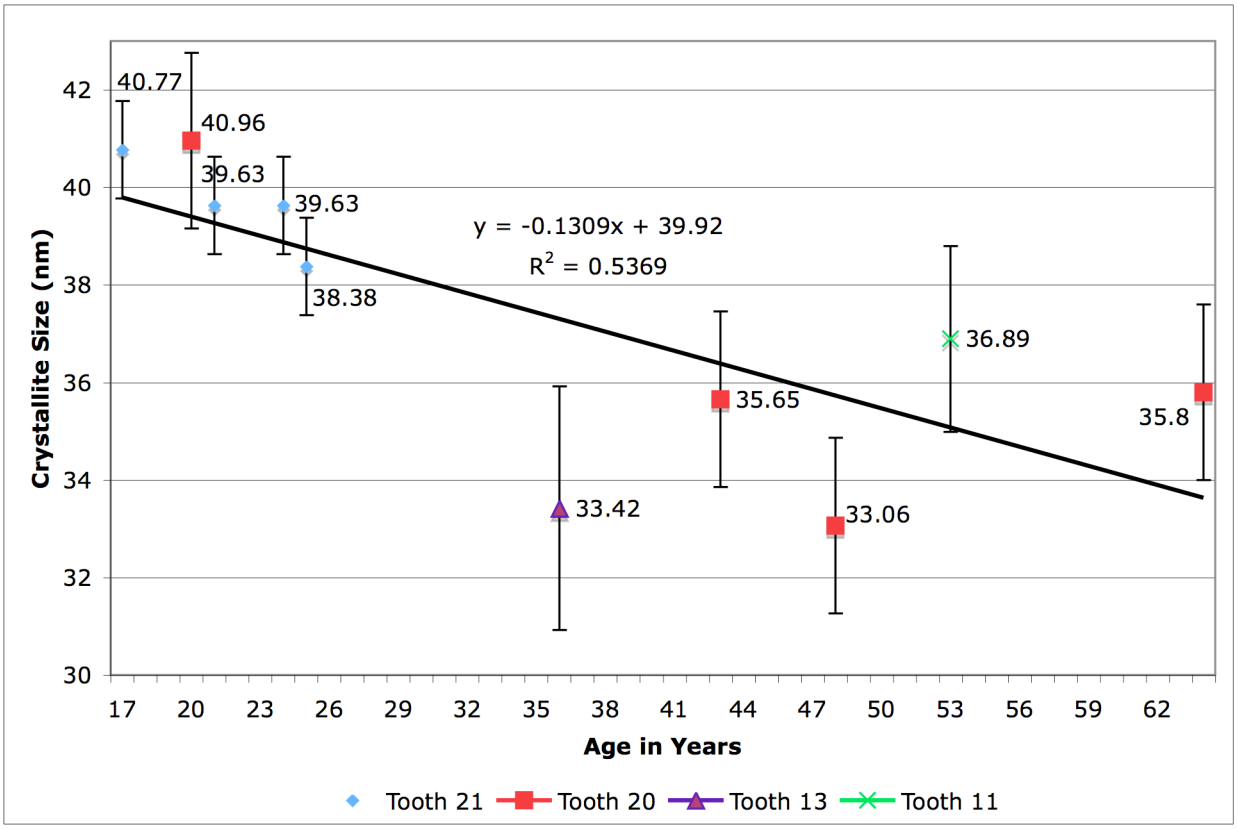

Figure 4.3 Graph Showing Age and Crystallite Size Correlation for Peak (002) in Single Peak Method for all of the Human Samples with Linear Trend Line and Error.

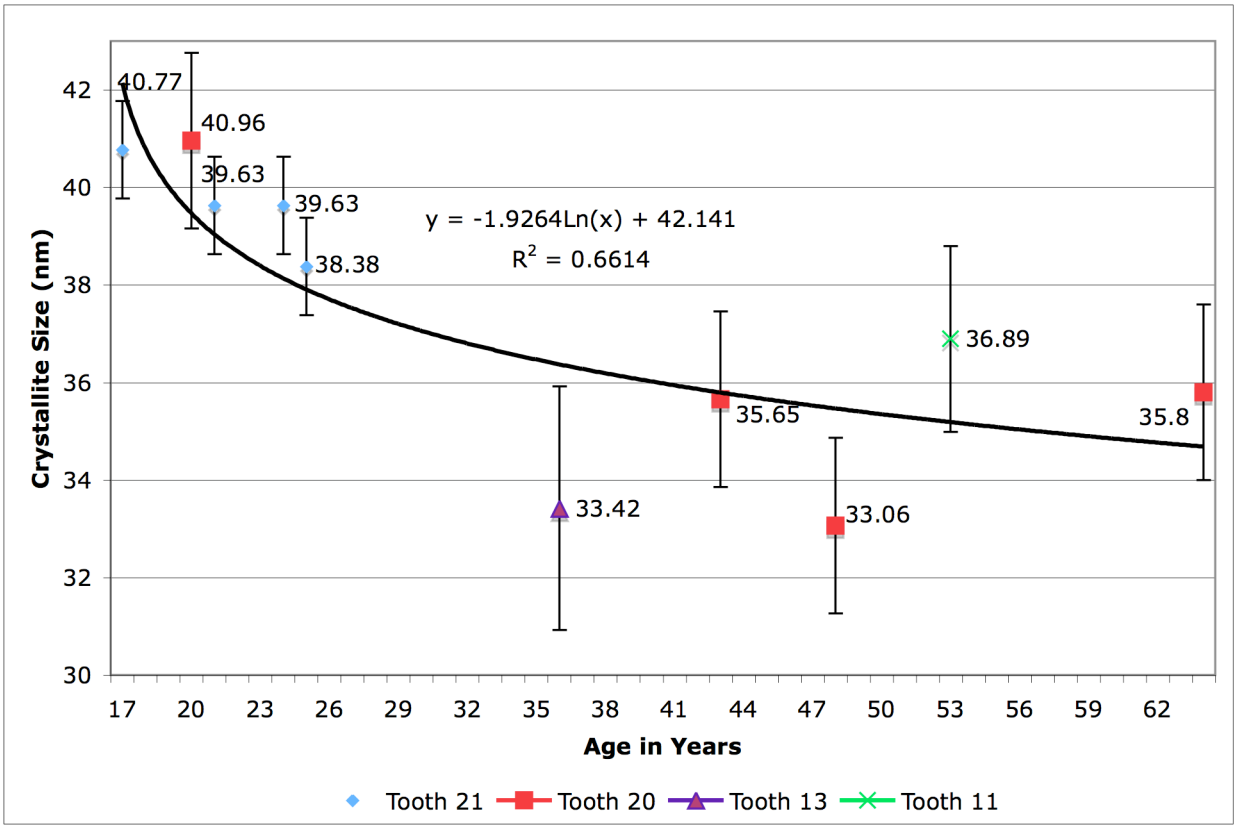

Figure 4.4 Graph Showing Age and Crystallite Size Correlation for Peak (002) in Single Peak Method for all of the Human Samples with Logarithmic Trend Line and Error.

The application of the single peak analysis for the resolved (211), (112), and (300) peaks from the peak decomposition is illustrated in Figures 4.5, 4.6, and 4.7, respectively. The data for the single peak analysis of the (211) peak result in a positive slope (0.0478) in the regression formula, which indicates a trend toward an increase in crystallite size with age. However, the line is not a good fit for the data because the R^2 value is 0.026. The regression formula for the (112) peak gives a negative slope at -0.0743 and an R^2 value of 0.0962. The regression formula for the (300) peaks also shows a negative slope (-0.378) and an R^2 of 0.0121. The slopes for both analyses indicate a decrease in crystallite size with increased age, but the R^2 values show that the lines are not a good fit for the data.

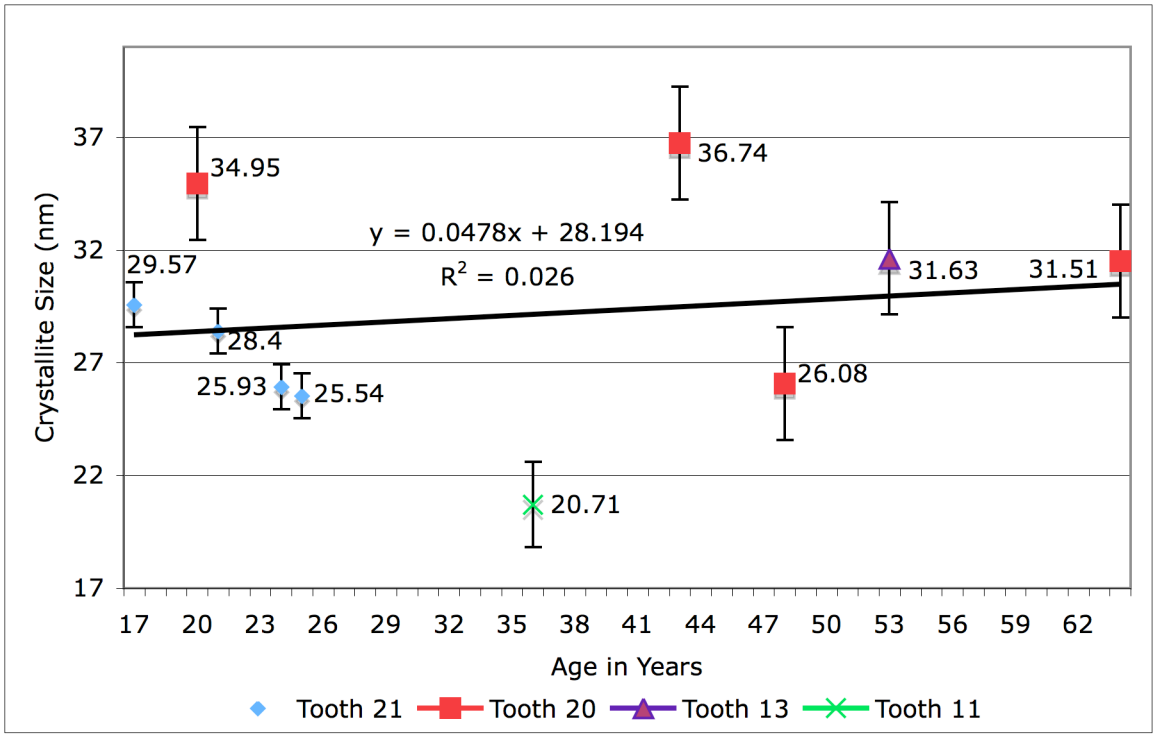

Figure 4.5 Graph Showing the Age and Crystallite Size Correlation with Error and Linear Regression for the Single Peak Method with the Resolved (211) Peak.

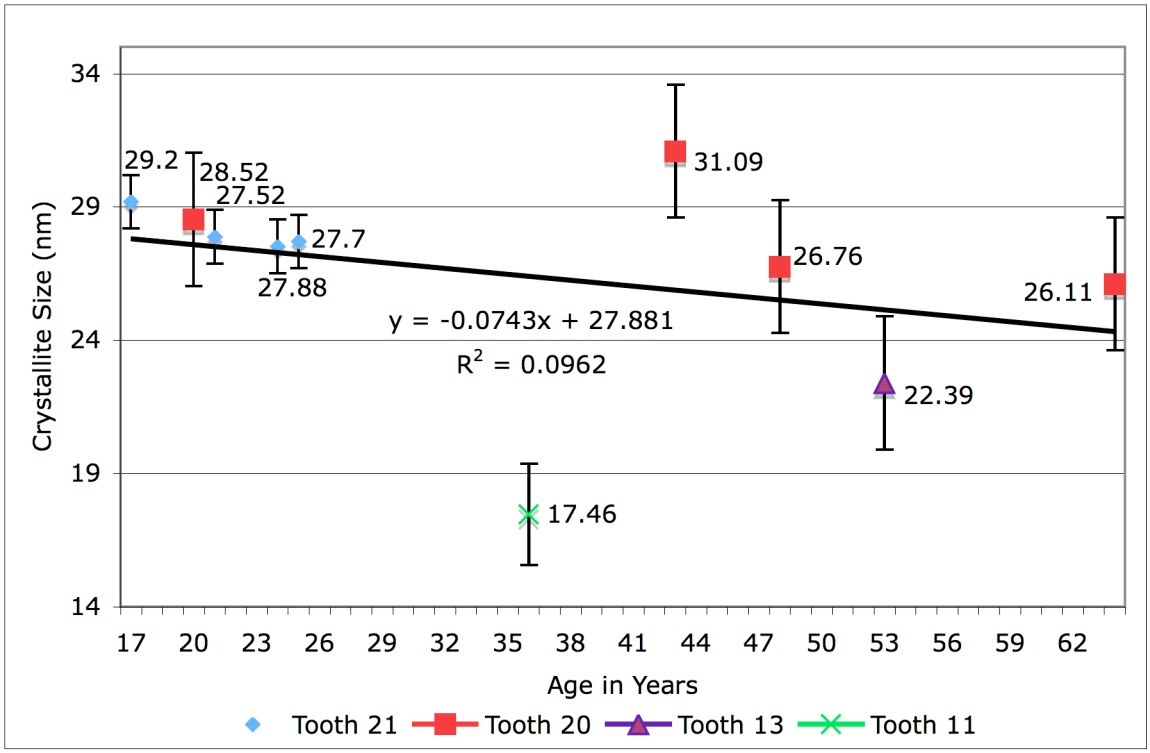

Figure 4.6 Graph Showing the Age and Crystallite Size Correlation with Error and Linear Regression for the Single Peak Method with the Resolved (112) Peak.

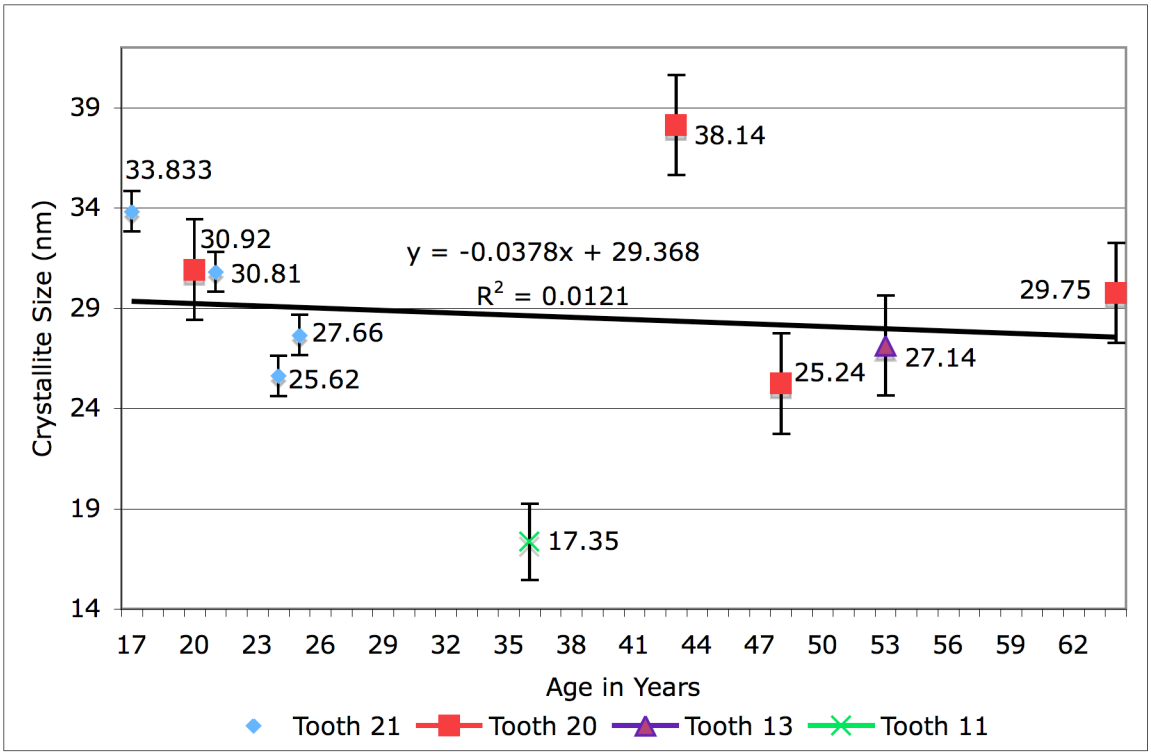

Figure 4.7 Graph Showing the Age and Crystallite Size Correlation with Error and Linear Regression for the Single Peak Method with the Resolved (300) Peak.

The multiple peak method resulted in variable data with very little correlation between age and crystallite size (Figure 4.8). The regression formula for the data has a small negative slope of -0.0215 and an R^2 value of 0.0063, which indicates the formula has almost no fit to the data. The major outliers for the data appear to be H10 (36 years old) and H2 (43 years old) as they are significantly farther away from the regression formula than the other data points.

4.3.2 Variation in Tooth Type

This study contained four tooth categories that included the maxillary left canine (#11), the mandibular left second premolar (#20), the maxillary left second premolar (#13), and the mandibular left first premolar (#21). The data for each of these tooth types were separated and

compared. Figure 4.3 is compiled with crystallite size data from the single peak method using the (002) peak for each tooth type.

There were four human samples for tooth type #21 and they are shown in Figure 4.9. These samples are closely related in age; the youngest is 17 years old and the oldest is 25 years old. The crystallite size for this set ranged from 40.77 nm to 38.38 nm. The progression of these four samples as they relate to age is a decrease in crystallite size. The regression formula for this set of samples has the largest negative slope at -0.2446 and an R^2 value of 0.8108 that demonstrates that the line is a good fit for the data.

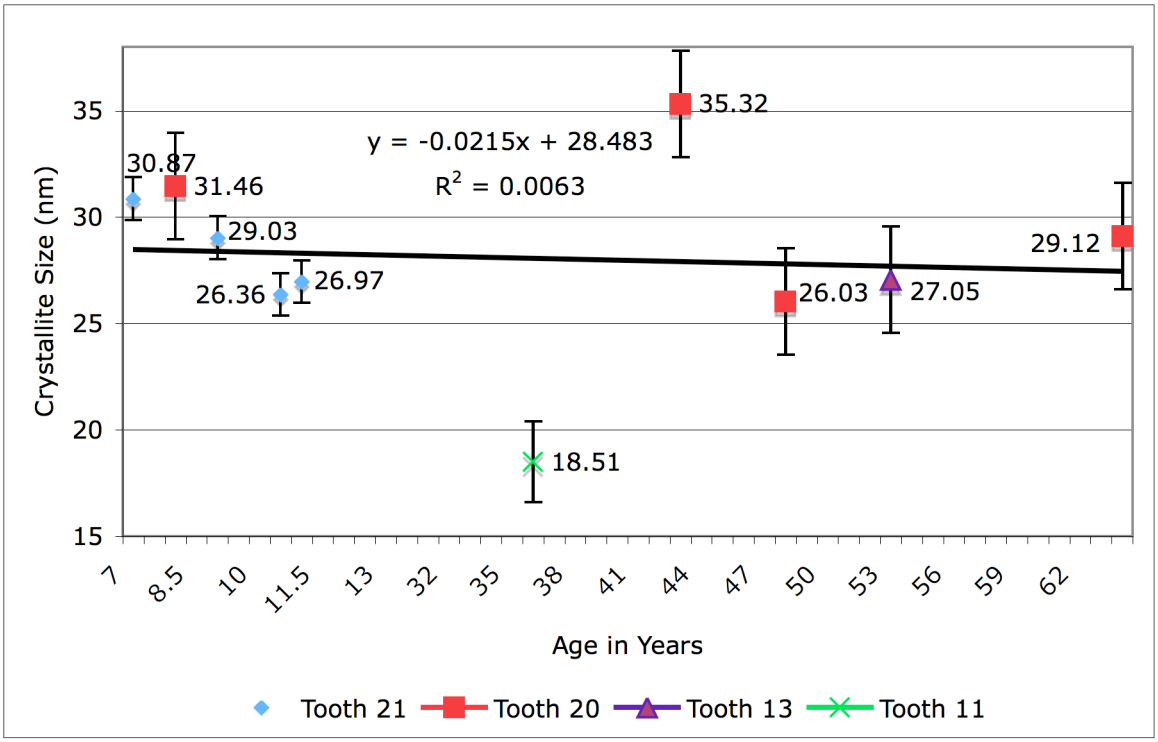

Figure 4.8 Graph Showing the Age and Crystallite Size Correlation and Linear Regression for the Multiple Peak Method with Peaks (211), (112), and (300).

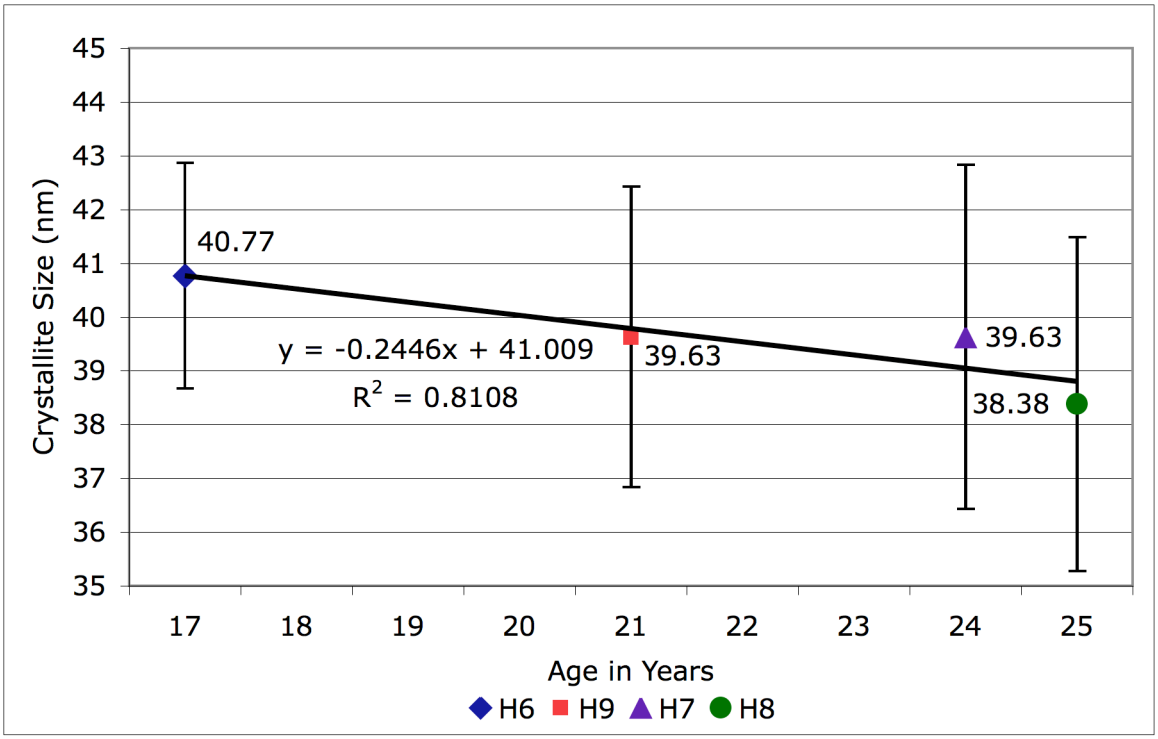

Figure 4.9 Graph Showing the Correlation Between Age and Crystallite Size in Tooth Type 21 with a Linear Regression of the Data.

The crystallite size to age correlation of tooth type #20 is shown in Figure 4.10. The slope of the regression formula for this data set was -0.1351 with an R^2 value of 0.551. The negative slope indicates a downward progression in crystallite size with increased age. The R^2 value is not large enough for the line to be considered a good fit, but it also indicates that the line has some correlation to the data.

Samples H5 and H10 were single examples of their respective tooth types. Figure 4.3 shows the relationship that these samples have with the other tooth types in the study sample. The age for sample H5 is significantly older than the other left second premolars at 53 years old. The crystallite size for this sample was calculated to be 36.89 nm, which is well below the four samples in the tooth type #20 set. An overall comparison for sample H10 was made because it is a maxillary left canine. The crystallite size for this sample (triangle) is shown in relation to the

other tooth types in Figure 4.6. It appears to be significantly smaller in crystallite size (33.42 nm) as compared to age (36 years old) than the other tooth types. The regression formula for the study sample yields an estimated crystallite size for that tooth type at age 36 to be about 37 nm, which is higher than the value for sample H10.

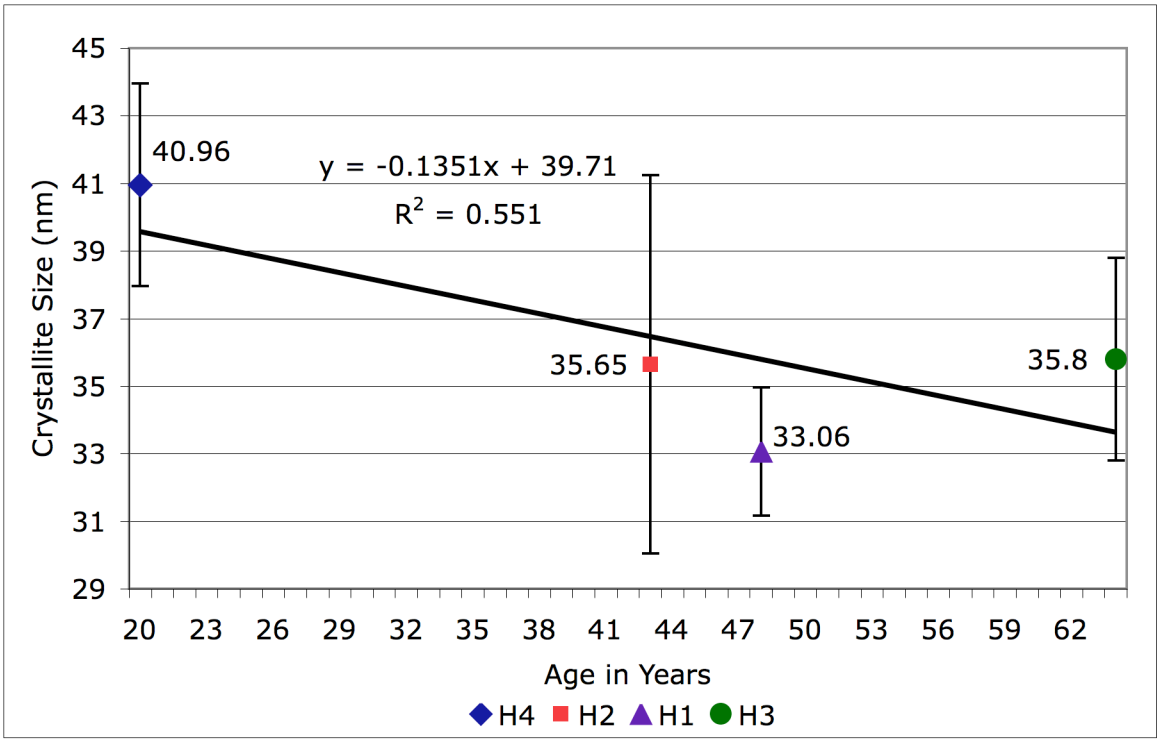

Figure 4.10 Graph Showing the Correlation Between Age and Crystallite Size in Tooth Type 20 with a Linear Regression of the Data.

CHAPTER FIVE: DISCUSSION AND CONCLUSIONS

The null hypothesis that there is no correlation between crystallite size and age could not be rejected, but the hypothesis that the crystallite size would increase with age could not be confirmed either. Based on the data for the (002) peak analyses, there is a trend toward decreased crystallite size with the increased age of an individual. These findings suggest that the converse of the hypothesis is true. An alternative hypothesis that the crystallite size of the hydroxylapatite in teeth will decrease as an individual ages was established. The general trend found in this research toward the reduction of crystallite size with increased age supports the alternative hypothesis.

A few generalizations can be made about the relationship between age and crystallite size. Due to the high number of young individuals present in this sample population, it is possible to see the slight changes in crystallite size in individuals between the age of 17 and 25. All of these samples within this age range had a crystallite size of between 40.77 nm and 38.38 nm with only a difference of 2.39 nm over those eight years. None of samples aged above 28 in this study fell above the 38.38 nm crystallite size threshold. The samples aged 36 to 64 years old ranged from 36.89 nm to 33.06 nm, but the oldest sample was not the lowest crystallite size and the youngest was not the largest crystallite size.

The single peak method with the use of peak (002) was shown to be the most useful method for analysis. The (211), (112), and (300) peaks that were analyzed with the single peak method produced results that had regression formulas with a poor fit for the data. This was due to the presence of two anomalous samples or outliers (H10 and H2) in the data. The multiple peak method produced results similar to the resolved individual peaks because this method was calculated using the averages of the three peaks. The major obstacle with analyzing decomposing overlapped peaks and using the resulting resolved peaks was establishing the best possible base line. The amount of definition that the grouped peaks had in the pattern also played a part in the

decomposition of the peaks. Strongly defined peaks within a pattern proved to produce decomposed peaks that had almost identical values for FWHM, and less defined peaks tended to yield a mixture of large and small decomposed peaks and variable FWHM values.

All of the data in this study were analyzed using linear regression, but a logarithmic regression was also applied to the human tooth samples (Figure 4.4). This regression model proved to be a slightly better fit for the data (R^2=0.6614) over the linear regression (R^2=0.5369). This may be an indication that the correlation between crystallite size and age is highest when an individual is relatively young; with age, the correlation appears to be weaker. More samples are needed to confirm a better fit with a logarithmic formula. A logarithmic regression applied to the data for the decomposed peaks did not yield higher R^2 values than the linear regressions illustrated in Figures 4.5 to 4.10 and were not applied to the analysis in this study.

The comparison of all of the human samples for an overall evaluation of the relationship between crystallite size and age was important for establishing general trend in the data with a regression formula. Due to some inconsistencies in the trend, it became apparent that tooth type was a vitally important factor in this study. As was shown with the second set of pig samples (PC1, PC2, and PC3), the age of one tooth is different than the age of another tooth in the same mouth due to differences in tooth development times. If the crystallite size of hydroxylapatite does change with age, mandibular first premolars (#21) will develop first at around 10.4 to 10.7 years old; maxillary second premolars (#13) will develop second at 11.0 to 11.2 years old; mandibular second premolars (#20) will develop during or after tooth #13 at 11.0 to 11.3 years old; and maxillary canines (#11) will develop at 11.0 to 11.6 years old (Carlos and Gittelsohn 1965). When the average age of each tooth eruption is accounted for and subtracted from the chronological age of the samples, the resulting data (Figure 5.1) showed very similar results to Figure 4.3. The R^2 value of 0.5165 for the data compiled in Figure 5.1 is slightly less than that of

the data that did not account for the average age of eruption (R^2=0.5369). This suggests that the regression formula for the data in Figure 4.3 has a better fit than the adjusted age data.

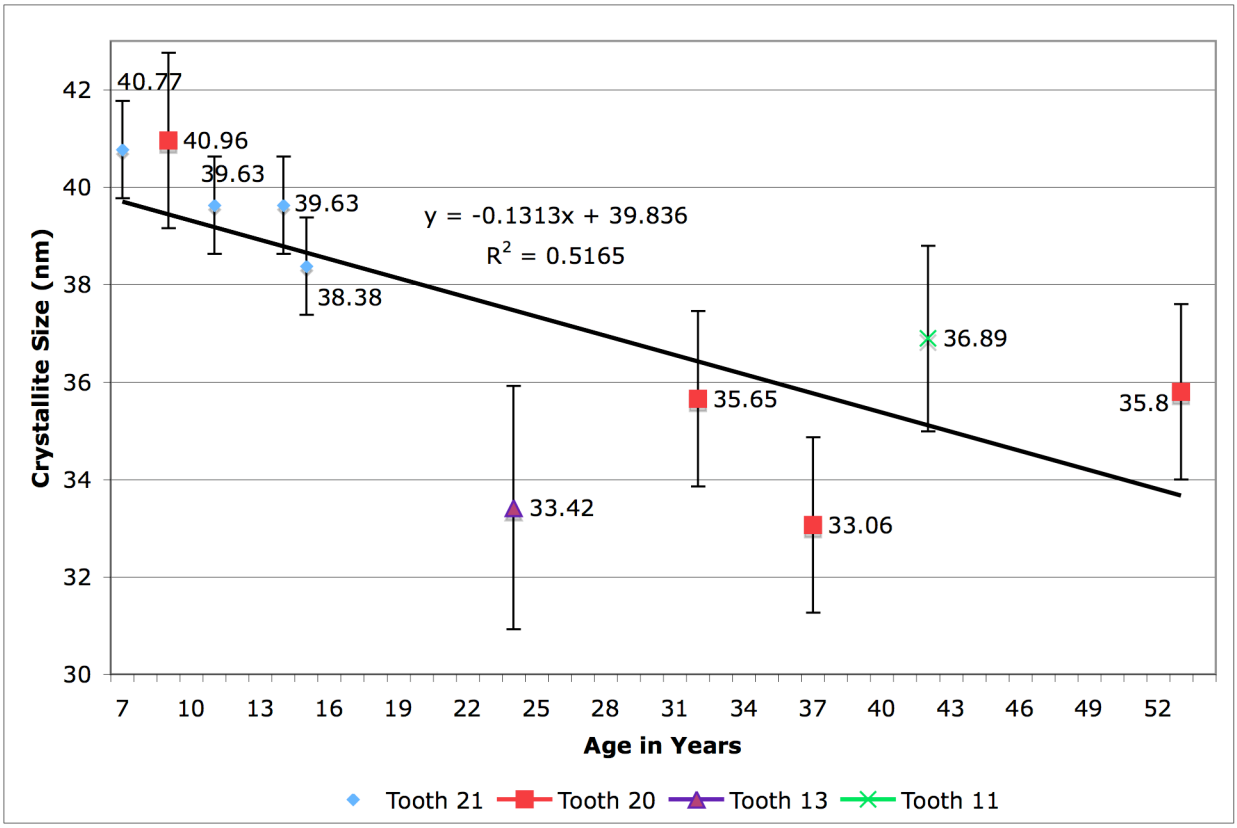

Figure 5.1 Graph Showing Age and Crystallite Size Correlation with Average Age of Eruption Subtracted from the Chronological Age for Peak (002) in Single Peak Method for all of the Human Samples with Linear Trend Line and Error.

The results from the three teeth collected from Pig C show that there are differences in crystallite size within an individual. Figure 4.1 illustrates this difference in eruption time and crystallite size. The difference in crystallite size between PC2 and PC3 is not statistically significant to an interval of 5% (P=0.14), but does fall within a 95% confidence interval for the data. Replication of this study is needed to establish clear differences among types of teeth.

The sample set for tooth #21 (mandibular first premolar) was very close in age and only subtle differences in crystallite size were noted. For the four representatives of this tooth type, a decrease in size of 2.39 nm with an age increase of eight years was noted. Figure 4.7 shows a

general descending trend that corresponds to the overall trend for all tooth types as illustrated in Figure 4.6. This tooth type showed the best results for a direct decrease in crystallite size with increased age. This may be due to the close proximity in age of each sample in this set.

The sample set for tooth #20 had a very wide range of ages and the differences were more pronounced with a decrease in size of 7.9 nm, for an increase of 28 years. With the exception of sample H3 (age 64), there was a clear decrease noted with increased age as shown in Figure 4.8. Sample H3 had no visible abnormalities and could be an outlier for the sample population. Sample H4 (age 20) had a very dark stained root, but it falls in with the other samples that are aged around 20 years (Figure 4.6).

Sample H10 had the potential to be the youngest or the second oldest of all of the teeth in this study. The crystallite size for H10 is 33.42 nm at a chronological age of 36 years. This age puts this tooth at the second smallest crystallite size for all of the human samples and about 4.5 years below the mean age for the study sample (40.5 nm). H10 also exhibited a high amount of dental attrition. It is unknown how attrition will affect the results, and this phenomenon requires further study. A more comprehensive study of canine tooth crystallite size is needed to determine the relationship between crystallite size and age in canines. However, when compared to the other two sample sets (figure 4.6), evidence supports the idea that types of teeth will have different crystallite size progression.

Sample H5 and the sample set for tooth #20 are all second premolars. As noted above, the mandibular and maxillary tooth types can develop at different times. H5 was one of the oldest samples at 53 years old and had a crystallite size of 36.89 nm. If H5 is placed in the tooth #20 samples set, the progression toward a decreased crystallite size with increased age was not supported. This is an example of how tooth development is an important factor in this analysis.

Table 2.1 shows that maxillary and mandibular second premolars can develop as slightly different times, which could make the chronological ages for each tooth type different.

The major outliers in the study sample proved to be H10, H2, and H1. Figures 4.5 to 4.7 show H10 (36 years old) and H2 (43 years old) significantly below and above the regression line, respectively, in each figure. Figures 4.3 and 4.4 show H10 (36 years old) and H1 (48 years old) well below both the linear and logarithmic regression in each respective figure. Sample H10 is a canine and the only human tooth sample in the study that is not a premolar. It was also the only tooth in the study sample that exhibited considerable amounts of dental attrition. The combination of tooth type and attrition could account for the sample's status as an outlier. No anomalies were noted for samples H1 and H2, and the only factor that separates these samples from the rest of the study sample is age. They are the only samples with a chronological age between 40 and 50 years. Sample H5 (53 years old) was the only sample that had a carious lesion and dental calculus, but it is not considered an outlier because it fit into the regression formula for all of the analyses.

The first three pig samples (Pig 1, 2, and 3) were collected, processed, and analyzed in order to establish the viability of the technique and analysis. This researcher did not know initially whether a tooth would yield enough processed sample to be able to load into a sample holder to analyze in the XRD. The initial weights of the three pig teeth (P1, P2, and P3) were below the typical amount of 2 grams that is suggested for proper sample loading. During processing, the samples lost very little weight and took on a light and feathery consistency that increased the overall volume. Loading the sample into the sample holder only required about half of the total volume for each sample.

The natural formations of secondary and tertiary dentin in teeth are important processes to be considered in this study. The development of secondary dentin, although slow, may have a contributing role in the reduction of the mean crystallite size found in this research. Tertiary

dentin forms more rapidly and in response to an injury or some other external stimuli. Sample H5 was the only sample in this study to have a carious lesion, which might have had tertiary dentin formation. Future research is needed to study the effects of secondary and tertiary dentin on the mean crystallite size of the hydroxylapatite within a tooth.

The appearance of quartz in all of the samples in this research was inconsistent with the composition of bone in other studies (Jansen et al. 1991; McPherson et al. 1995), but it is unknown whether these studies also identified quartz and chose not to report it in their findings. If the quartz is unique to this study, the presence of quartz was most likely due to contamination during preparation or a natural part of tooth development. The quartz peaks were identified and removed from the data set. No interference between the quartz peaks and the hydroxylapatite peaks seems to exist; therefore, the quartz peaks were not included in the data portion of this analysis.

This research was conducted on a very limited number of samples. More research is needed to be able to establish the exact crystallite size to age correlation and to determine the cause of the decrease in crystallite size with increased age. Although limited in scope, this study shows that changes take place in teeth with increased age. The evidence for the decreased crystallite size with increased age was exemplified in the 17 to 25 year old samples. The fact that none of the samples above the age of 28 approached the four young samples in crystallite size provides good evidence for the possibility for future research to demonstrate a clear trend in decreased crystallite size in older individuals. These data also show that determining a precise age based on crystallite size may not be achievable, but that an estimated age range may be the best possible result of XRD analysis of the crystallite size in teeth.

REFERENCES CITED

Augat, P., and Schorlemmer, S.
2006. "The role of cortical bone and its microstructure in bone strength." *Age and Ageing* 35-S2:ii27-ii31.

Baltag, I., Watanabe, K., Kusakari, H., Taguchi, N., Miyakawa, O., Kobayashi, M., and Ito, N.
2000. "Long-term changes of hydroxylapatite-coating dental implants." *Journal of Biomedical Materials Research* 53(1):76-85.

Bass, W.M.
2005. *Human osteology: A laboratory and field manual.* Missouri Archaeological Society, Columbia, Missouri.

Beckett, S., and Rogers, K.
2008. "Species Identification of Fragmented Bone: Evaluation of a New Method of Pyrolysis and X-ray Diffraction Analysis." *American Academy of Forensic Science 60th Anniversary Scientific Meeting*, February 18-23, 2008, Washington, DC.

Bodkin, T.E., and Mies, J.W.
2008, "X-ray diffraction (XRD) analysis of human cremains and concrete." *American Academy of Forensic Science 60th Anniversary Scientific Meeting*, February 18-23, 2008, Washington, DC.

Byers, S.N.
2008. *Introduction to forensic anthropology.* Pearson Education, Boston.

Carlos, J.P., and Gittelsohn, A.M.
1965. "Longitudinal studies of the natural history of caries, I: Eruption patterns of the permanent teeth." *Journal of Dental Research* 44(3):509.

Catts, E.P., Goff, M.L.
1992. "Forensic entomology in criminal justice." *Annual Review of Entomology*. 37:253-72.

Chang, C., Huang, J., Xia, J., and Ding, C.
1999. "Study on crystallization kinetics of plasma sprayed hydroxylapatite coating." *Ceramics International* 25(5):479-483.

Chang, C., Shi, J., Huang, J., Hu, Z., and Ding, C.
1998. "Effects of power level on characteristics of vacuum plasma sprayed hydroxypatite coating." *Journal of Thermal Spray Technology* 7(4):484-488.

Chatterji, S. and J. W. Jeffery.
1968. "Changes in structure of human bone with age." *Nature* 219:482-484.

De Jong, W.F.
1926. “La Substance minerale dans les os.” *Recueil des Travaux Chimie* 45:445-448.

Dupras, T.L., Schultz, J.J., Wheeler, S.M., and Williams, L.J.
2005. *Forensic recovery of human remains: Archaeological approaches.* Taylor & Francis, Boca Raton.

Gineste, L., Gineste, M., Ranz, X., Ellefterion, A., Guilhem, A., Rouquet, N., and Frayssinet, P.
1999. “Degradation of hydroxylapatite, fluorapatite, and fluorhydroxyapatite coatings of dental implants in dogs.” *Journal of Biomedical Materials Research* 48(3):224-234.

Glusker, J.P., Lewis, M., and Rossi, M.
1994. *Crystal structure analysis for chemists and biologists*. VCH Publishers, New York.

Handschin, R.G., and Stern, W.B.
1992. “Crystallographic lattice refinement of human bone.” *Calcified Tissue International* 51(2):111-120.

Hebbar, K.R.
2007. *Basics of X-ray diffraction and its applications.* IK International Publishing: New Delhi.

Hillson, S.
1996. *Dental anthropology*. Cambridge University Press, New York.

Jansen, J.A., van de Waerden, J.P.C.M., Wolke, J.G.C., and De Groot, K.
1991. “Histological evaluation of the osseous adaptation to titanium and hydroxyapatite-coated titanium implants.” *Journal of Biomedical Materials Research* 25(8):973-989.

Kirkham, J., Brooks, S.J., Shore, R.C., Bonass, W.A., Smith, D.A.M., Wallwork, and M.L., Robinson, C.
1998. “Atomic force microscopy studies of crystal surface topology during enamel development.” *Connective Tissue Research* 38:91-100.

Kuttler, Y.
1959. “Classification of dentine into primary, secondary, and tertiary.” *Oral Surgery, Oral Medicine, and Oral Pathology* 12(8):996-9

Lovejoy, C.O., Meindl, R.S., Mensforth, R.P., Barton, T.J.
1984. “Mulitfactorial determination of skeletal age at death: A method and blind tests of its accuracy.” American *Journal of Physcial Anthropology* 6(1):1-14.

Magnell, O., and Carter, R.
2007. “The chronology of tooth development in wild boar – A guide to age determination of linear enamel hypoplasia in prehistoric and medieval pigs.” *Veterinarija Ir Zootechnika* 40(62):51-81.

Materials Data
2001. Jade XRD Pattern Processing. Materials Data, Inc.

Matschke, G.H.
1967. "Aging European wild hogs by dentition." *Journal of Wildlife Management* 31(1):109-113.

McFee, A.F., and Banner, M.W.
1969. "Inheritance of chromosome number in pigs." *Journal of Reproduction and Fertility* 18:9-14.

McPherson, R., Gane, N., and Bastow, T.J.
1995. "Structural characterization of plasma-sprayed hydroxylapatite coatings." *Journal of Materials Science: Materials in Medicine* 6(6):327-334.

Meier, M.
2004. "Crystallite size measurement using X-ray diffraction." *EMS-162L Laboratory Manual* University of California Davis. <http://www.matsci.ucdavis.edu/MatSciLT/EMS-162L/Files/XRD-CSize1.pdf>

Meneghini, C., et al.
2003. "Rietveld refinement on X-ray diffraction patterns of bioapatite in human fetal bones." *Biophysical Journal* 84:2021-2029.

Ousley, S.D., and Jantz, R.C.
2005. FORDISC 3.0 Personal Computer Forensic Discriminant Functions. The University of Tennessee.

Pfeiffer, S., Lazenby, R., and Chang J.
1995. "Brief communication: Cortical remodeling data are affected by sampling location." *American Journal of Physical Anthropology* 96:89-92.

Robinson, J.W., Skelly Frame, E.M., and Frame, G.M.
2005. *Undergraduate Instrumental Analysis*. Marcel Dekker, New York.

Robinson, R.A., and Watson, M.L.
1955. "Collagen-crystal relationships in bone as observed in the electron microscope. III. Crystal and collagen morphology as a function of age." *Annals of the New York Academy of Science* 60:596-629.

Rusu, V.M., Ng, C.H., Wilke, M., Tiersch, B., Fratzl, P., and Peter, M.G.
2005. "Size-controlled hydroxyapatite nanoparticles as self-organized organic-inorganic composite materials." *Biomaterials* 26:5414-5426.

Sidaway, D.A.
1979. "A microbiological study of dental calculus." *Journal of Periodontal Research* 14(2):167-172.

Thamaraiselvi, T.V., Prabakaran, K., and Rajeswari, S.
2006. “Synthesis of hydroxyapatite that mimic bone mineralogy.” *Trends in Biomaterials & Artificial Organs* 19(2):81-83.

Trautz, O.R.
1955. “X-ray diffraction of biological and synthetic apatites.” *Annals of the New York Academy of Science* 60:698-713.

Verdelis, K., Lukashova, L., Wright, J.T., Mendelsohn, R., Peterson, M.G.E., Doty, S., and Boskey, A.L..
2007. “Maturational changes in dentin mineral properties.” *Bone* 40(5):1399-407.

Vetter, U., Eanes, E.D., Kopp, J.B., Termine, J.D., and Robey, P.G.
1991. “Changes in apatite crystal size in bones of patients with osteogenesis imperfecta.” *Calcified Tissue International* 49:248-250.

White, T.D., and Folkens, P.A.
2005. *The human bone manual*. Elsevier Academic Press, New York.

Woelfel, J.B., and Scheid, R.C.
2003. *Dental anatomy: Its relevance to dentistry.* Lippincott Willaims & Wilkins, Baltimore.

Wopenka, B., and Pasteris, J.
2005. “A mineralogical perspective on the apatite in bone.” *Materials Science and Engineering* 25:131-143.

Ye, F., Guo, H., and Zhang, H.
2008. “Biomimetic synthesis of oriented hydroxyapatite mediated by nonionic sufacntants.” *Nanotechnology* 19:245605.

APPENDIX: RAW DATA

Sample	(hkl)	@ 2-Theta	d(A)	FWHM
P1	(002)	25.879(0.010)	3.4400(0.0027)	0.294(0.019)
P2	(002)	25.851(0.010)	3.4436(0.0026)	0.302(0.017)
P3	(002)	25.908(0.012)	3.4361(0.0032)	0.343(0.020)
PC1	(002)	25.820(0.012)	3.4477(0.0031)	0.329(0.022)
PC2	(002)	25.824(0.017)	3.4471(0.0044)	0.333(0.032)
PC3	(002)	25.852(0.021)	3.4435(0.0054)	0.288(0.028)
H1	(002)	25.833(0.008)	3.4460(0.0021)	0.258(0.015)
	(211)	31.682(0.014)	2.8219(0.0024)	0.331(0.033)
	(112)	32.121(0.020)	2.7843(0.0034)	0.323(0.060)
	(300)	32.793(0.021)	2.7288(0.0034)	0.343(0.036)
H2	(002)	25.840(0.015)	3.4451(0.0038)	0.219(0.031)
	(211)	31.672(0.012)	2.8227(0.0020)	0.243(0.037)
	(112)	32.109(0.014)	2.7853(0.0024)	0.267(0.059)
	(300)	32.804(0.010)	2.7279(0.0016)	0.267(0.016)
H3	(002)	25.845(0.008)	3.4443(0.0021)	0.241(0.016)
	(211)	31.702(0.011)	2.8201(0.0019)	0.274(0.023)
	(112)	32.105(0.021)	2.7856(0.0035)	0.331(0.067)
	(300)	32.806(0.015)	2.7277(0.0025)	0.291(0.031)
H4	(002)	25.835(0.007)	3.4457(0.0019)	0.208(0.015)
	(211)	31.691(0.007)	2.8211(0.0012)	0.238(0.015)
	(112)	32.141(0.013)	2.7826(0.0021)	0.303(0.020)
	(300)	32.800(0.010)	2.7282(0.0015)	0.274(0.015)
H5	(002)	25.879(0.007)	3.4400(0.0019)	0.231(0.015)
	(211)	31.728(0.011)	2.8179(0.0020)	0.293(0.022)
	(112)	32.152(0.020)	2.7817(0.0033)	0.331(0.064)
	(300)	32.838(0.012)	2.7251(0.0019)	0.264(0.024)
H6	(002)	25.881(0.056)	3.4397(0.0146)	0.238(0.014)
	(211)	31.732(0.013)	2.8176(0.0022)	0.292(0.022)
	(112)	32.156(0.019)	2.7813(0.0032)	0.296(0.056)
	(300)	32.833(0.013)	2.7255(0.0022)	0.261(0.026)
H7	(002)	25.877(0.008)	3.4402(0.0020)	0.215(0.017)
	(211)	31.740(0.015)	2.8169(0.0026)	0.333(0.039)
	(112)	32.149(0.021)	2.7819(0.0036)	0.314(0.072)
	(300)	32.837(0.022)	2.7252(0.0036)	0.338(0.042)
H8	(002)	25.872(0.009)	3.4409(0.0023)	0.222(0.018)
	(211)	31.726(0.015)	2.8180(0.0025)	0.338(0.034)
	(112)	32.128(0.022)	2.7837(0.0037)	0.312(0.078)
	(300)	32.825(0.019)	2.7262(0.0031)	0.313(0.036)

H9	(002)	25.830(0.008)	3.4464(0.0020)	0.222(0.016)
	(211)	31.703(0.012)	2.8200(0.0020)	0.304(0.027)
	(112)	32.112(0.021)	2.7851(0.0035)	0.310(0.063)
	(300)	32.800(0.013)	2.7282(0.0022)	0.281(0.024)
H10	(002)	25.925(0.009)	3.4339(0.0023)	0.278(0.017)
	(211)	31.816(0.014)	2.8103(0.0025)	0.411(0.134)
	(112)	32.193(0.050)	2.7782(0.0084)	0.494(0.199)
	(300)	32.831(0.053)	2.7257(0.0086)	0.484(0.227)

VITA

Teresa Veronica Wilson was born in May 1984, on the Paiute-Shoshone Reservation in Lone Pine, California. She graduated from Northern Arizona University in May, 2007, with a Bachelor of Arts in anthropology and a minor in criminal justice. In August 2007, Teresa entered graduate school in the Geography and Anthropology Department at Louisiana State University. Upon completion of a Master of Arts degree, she plans to teach and pursue a doctoral degree in anthropology.